

Supporting Information

Pronounced effects on switching efficiency of diarylcycloalkenes on cycloalkene ring contraction

Dmytro Sysoiev,^a Tetyana Yushchenko,^a Elke Scheer,^b Ulrich Groth,^a Ulrich E. Steiner^a, Thomas E. Exner,^{a*} and Thomas Huhn^{a*}

[a] *Fachbereich Chemie
Universität Konstanz
D-78457 Konstanz
Germany
Tel: +49-7531-884424
E-mail: thomas.exner@uni-konstanz.de; thomas.huhn@uni-konstanz.de*

[b] *Fachbereich Physik
Universität Konstanz
D-78457 Konstanz*

Contents:

- 1. Synthetic Work**
- 2. UV/vis-Spectra**
- 3. NMR-Spectra**
- 4. Crystallographic Data**
- 5. Quantum Mechanical Calculation**
- 6. References**

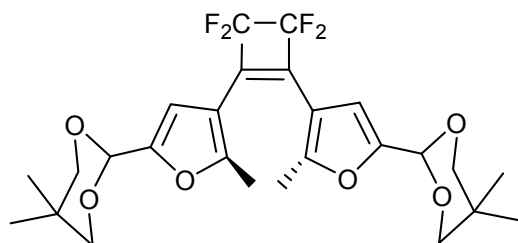
1. Synthetic Work

General remarks:

All reactions were carried out under an atmosphere of dry nitrogen in oven-dried glassware unless otherwise noted. All TLCs were performed on Polygram Sil G/UV₂₅₄ plates (MACHEREY-NAGEL GmbH & Co. KG, Düren). UV-light of 254 nm was used for detection. Elemental analyses were performed on a CHN-analyser Heraeus (CHN-O-RAPID) by the Microanalysis laboratory of Konstanz University. IR-spectra were recorded on a Perkin-Elmer 100 Series FT-IR spectrometer with ATR-unit. GC/MS-data were recorded on an Agilent GC/MS 7890A/5975C instrument (EI, 70 eV). HRMS ESI/FT-ICR spectra were recorded on a Bruker APEX II FT/ICR instrument. FAB MS was performed on a Finnigan MAT 8200 instrument. UV-Vis spectra were recorded on a Cary 50 spectrophotometer. NMR spectra were recorded on a Bruker Avance DRX600 (600 MHz) and a Jeol ECP-Eclipse 400 (400 MHz).

Materials:

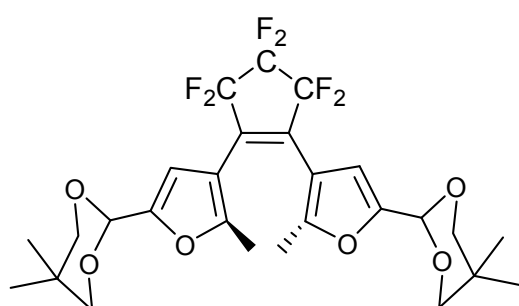
Starting materials and solvents used were purchased from Sigma-Aldrich, Fluka, Acros, ABCR and Fluorochem. Perfluorocyclobutene (25 g) was dissolved in dry THF (57 ml) before use.



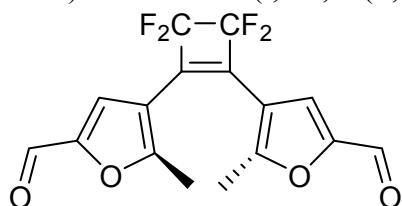
1,2-Bis(5-(5,5-dimethyl-1,3-dioxan-2-yl)-2-methylfuran-3-yl)perfluorocyclobutene (C4F-NPA) (1):

To a solution of 4-bromo-5-methyl-2-furaldehyde neopentyl acetal^[1] (3.2 g, 11.7 mmol) in dry THF (20 ml) *t*BuLi (17.72 ml, 28 mmol, 1.6 M/hexane) was added dropwise at -78°C under N₂ and the reaction mixture was stirred for 30 min at -78°C. A solution of hexafluorocyclobutene (0.95 g, 5.86 mmol) in dry THF (1 ml) was added dropwise and the reaction mixture was brought to rt and stirred overnight. After quenching with aqueous NH₄Cl, the organic solvent was removed in vacuo, water (100 ml) was added and the oily residue was extracted with diethyl ether (3x100 ml). The combined organic phases were dried with MgSO₄ and the solvent was removed in vacuo yielding brown oil. After column chromatography, 1.7 g of crude **1** was obtained as yellow oil and was used for the next step. The compound was obtained in an analytically pure form as yellowish crystals after recrystallization from *n*-hexane and subsequent sublimation. Yield: 56%. R_f = 0.45 (silica, hexanes/EtOAc 2:1); m. p. 184–186°C; ¹H NMR (400 MHz, CDCl₃, 25°C): δ = 0.78 (s, 6H; CH₃), 1.25 (s, 6H; CH₃), 2.41 (s, 6H, CH₃ (aryl)), 3.58 (d, ²J(H,H)=10.9 Hz; 4H; CH₂), 3.73 (d, ²J(H,H)=11.3 Hz; 4H; CH₂), 5.39 (s, 2H; CH (acetal)), 6.50 ppm (s, 2H; Ar-H (furyl)); ¹³C NMR (100 MHz, CDCl₃, 25°C): δ = 13.40 (CH₃ (furyl)), 22.61 (CH₃), 22.80 (CH₃), 30.29 (CMe₂), 77.31 (CH₂), 95.41 (CH (acetal)), 107.86 (C-4), 109.52 (C-3), 118.51 (m, CF₂), 135.16 (m, CCF₂), 150.62 (C-5), 153.96 ppm (C-2); ¹⁹F NMR (376 MHz, CDCl₃, 25°C): δ = -110.48 (s, 4F); IR: ν = 2959, 2864, 1580, 1464, 1315, 1223, 1087 cm⁻¹; FAB-MS: *m/z*: 514 [M⁺], 343; HRMS calcd for C₂₆H₃₀F₄O₆ [M+1H]⁺: 515.2051; found: 515.1922; elemental analysis calcd (%) for C₂₆H₃₀F₄O₆: C 60.69, H 5.88; found: C 60.73, H 6.13. Closed form isomer of **1**: dark-orange oil; ¹H NMR (400 MHz, CD₃OD, 25°C): δ = 0.78 (6H, CH₃), 1.21 (6H, CH₃), 1.54 (s, 6H; CH₃), 5.20 (s, 2H; CH (acetal)), 5.85 ppm (s, 2H; CH (furyl)); ¹⁹F NMR (376 MHz, CD₃OD, 25°C): δ = -109.60 (m, 2F, ²J(F,C)=207 Hz), -113.78 ppm (m, 2F, ²J(F,C)=207 Hz).

1. Synthetic Work



1,2-Bis(5-(5,5-dimethyl-1,3-dioxan-2-yl)-2-methylfuran-3-yl)perfluorocyclopentene (C5F-NPA): To a solution of 4-bromo-5-methyl-2-furaldehyde neopentyl acetal^[1] (2.41 g, 8.77 mmol) in dry THF (50 ml) *n*BuLi (6.1 ml, 9.76 mmol, 1.6 M/hexane) was added dropwise at -78°C under N₂ and the reaction mixture was stirred for 30 min at -78°C. A solution of octafluorocyclopentene (0.57 ml, 4.3 mmol) in dry THF (5 ml) was added dropwise over a period of 5 min and the reaction mixture was brought to rt and stirred overnight. After quenching with aqueous NH₄Cl, the organic solvent was removed in vacuo, water (100 ml) was added and the oily residue was extracted with diethyl ether (3x100 ml). The combined organic phases were dried with MgSO₄ and the solvent was removed in vacuo yielding brown oil. After filtering through a column filled with silica (hexanes/EtOAc 2:1 as eluent), 1.06 g of crude **C5F-NPA** was obtained as yellow oil. The compound was obtained in an analytically pure form as white crystals after recrystallization from *n*-hexane. Yield: 43%; m. p. 130–133°C; ¹H NMR (400 MHz, CDCl₃, 25°C): δ = 0.79 (s, 6H; CH₃), 1.28 (s, 6H; CH₃), 1.99 (s, 6H; CH₃ (furyl)), 3.59 (d, ²J(H,H)=10.9 Hz; 4H; CH₂), 3.75 (d, ²J(H,H)=11.3 Hz, 4H; CH₂), 5.39 (s, 2H; CH (acetal)), 6.47 ppm (s, 2H; Ar-H (furyl)); ¹³C NMR (100 MHz, CDCl₃, 25°C): δ = 13.65 (CH₃ (furyl)), 21.97 (CH₃), 23.09 (CH₃), 30.55 (C(CH₃)₂), 77.66 (CH₂), 95.75 (CH (acetal)), 108.35 (C-4), 109.71 (C-3), 110.81 (m, CF₂CF₂CF₂), 116.22 (m, CF₂CF₂CF₂), 132.43 (m, CCF₂), 150.45 (C-5), 153.42 ppm (C-2); ¹⁹F NMR (376 MHz, CDCl₃, 25°C): δ = -110.01 (t, ³J(F,F)=5.2 Hz, 4F; CF₂CF₂CF₂), -131.67 ppm (m, 2F; CF₂CF₂CF₂); IR: ν = 2962, 2855, 1395, 1275 cm⁻¹; FAB-MS: *m/z*: 565 [M+1]⁺; HRMS calcd for C₂₇H₃₀F₆O₆ [M+H]⁺: 565.2019; found: 565.2004; elemental analysis calcd (%) for C₂₇H₃₀F₆O₆: C 57.45, H 5.36; found: C 57.22, H 5.39. Closed form isomer of **C5F-NPA**: amber colored semi-solid; ¹H NMR (400 MHz, CDCl₃, 25°C): δ = 0.78 (s, 6H; CH₃), 1.23 (s, 6H; CH₃), 1.59 (s, 6H; CH₃ (furyl)), 3.53 (d, ²J(H,H)=11.3 Hz; 4H; CH₂), 3.72 (m, 4H; CH₂), 5.11 (s, 2H; CH (acetal)), 6.00 ppm (s, 2H; Ar-H (furyl)); ¹⁹F NMR (376 MHz, CDCl₃, 25°C): δ = -114.26 (t, 4F, ³J(F,F)=6.1 Hz; CF₂CF₂CF₂), -133.75 ppm (m, 2F; CF₂CF₂CF₂).

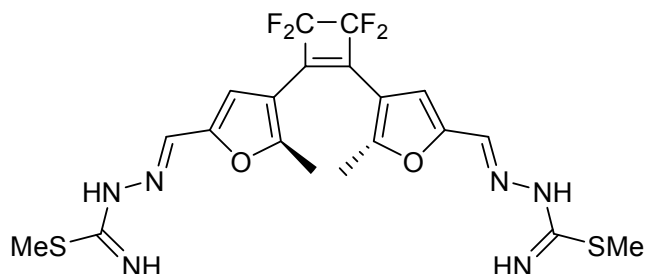


1,2-Bis(2-methyl-5-formylfuran-3-yl)perfluorocyclobutene (C4F-CHO) (2):

1 (0.5 g, 0.97 mmol) was dissolved in a THF/acetone mixture (20 ml each) and cooled to 10 °C. Conc. HCl (5 ml) was slowly added while maintaining the temperature between 10 – 15 °C. After complete addition, the solution was stirred at rt. and monitored by TLC. After complete deprotection the organic solvents were removed in vacuo and the residue was brought to pH=9 by adding aqueous NaHCO₃. After extraction with diethyl ether (3x50 ml) the combined organic fractions were dried with MgSO₄ and the solvent was removed in vacuo. The oily residue was purified by column chromatography, thus giving 0.3 g of **2** as brown oil. Analytically pure yellowish crystals of **2** were obtained after recrystallization from chloroform and subsequent sublimation. Yield: 90%. R_f = 0.27 (hexanes/EtOAc 2:1); darkens at 95°C, melts at 105°C; ¹H NMR (400 MHz, CDCl₃, 25°C): δ = 2.57 (s, 6H; CH₃), 7.24 (s, 2H; Ar-H), 9.63 ppm (s, 2H; CHO); ¹³C NMR (150 MHz, CDCl₃, 25°C): δ = 14.16 (CH₃), 111.62 (C-3), 118.19 (m, CF₂),

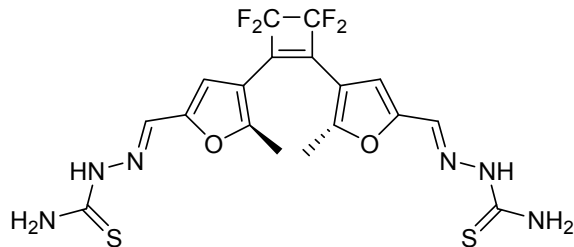
1. Synthetic Work

120.00 (CH (aryl)), 135.81 (m, CCF₂), 152.24 (C-5), 160.23 (C-2), 177.20 ppm (CHO); ¹⁹F NMR (376 MHz, CDCl₃, 25°C): δ = -110.05 (s, 4F); correlations confirmed by ¹H-¹³C-HSQC, ¹H-¹³C-HMBC, ¹⁹F-¹³C-HSQC and ¹⁹F-¹³C-HMBC experiments; IR: ν = 3122, 2828, 1671 (C=O), 1317, 1094 cm⁻¹; MS: *m/z*: 342 [M⁺]; HRMS calcd for C₁₆H₁₀F₄O₄ [M+1H]⁺: 343.0588; found: 343.0577; elemental analysis calcd (%) for C₁₆H₁₀F₄O₄: C 56.15, H 2.95; found: C 56.33, H 3.30.



1,2-Bis(2-methyl-5-((E)-(1-methylthio-1-iminomethylhydrazone)methyl)furan-3-yl)perfluorocyclobutene (C4F-MTSC) (3):

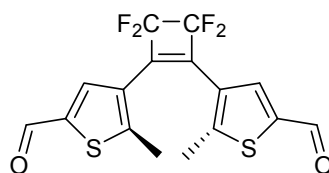
2 (50 mg, 0.15 mmol) and methylthiosemicarbazide (30 mg, 0.29 mmol) were dissolved in hot EtOH (5 ml) with a few drops of pure acetic acid. The reaction mixture was brought to reflux and stirred for 3 h. After cooling to rt it was poured into water (30 ml) and the precipitate was filtered off. After washing with cold EtOH (3 ml) and drying 71 mg of pale-yellow crystals were obtained. Yield: 94%. m. p. >190°C; ¹H NMR (400 MHz, [D₆]DMSO, 25°C): δ = 2.44 (s, 6H; CH₃), 2.99 (s, 6H; SCH₃), 7.07 (s, 2H; Ar-H (furyl)), 7.93 (s, 2H; HC-6), 8.28 (br, 2H; C=NH), 11.59 ppm (br, 2H; HNN); ¹³C NMR (100 MHz, [D₆]DMSO, 25°C): δ = 13.61 (CH₃), 30.92 (SCH₃), 110.26 (C-3), 111.76 (CH (furyl)), 119.04 (CF₂ (from ¹⁹F-¹³C-HSQC)), 130.86 (C=N), 149.46 (C-5), 155.91 (C-2), 177.58 ppm (C=N); ¹⁹F NMR (376 MHz, DMSO, 25°C): δ = -109.40 ppm (s); IR: ν = 3636, 3384, 3124, 2972, 1545, 1514, 1321, 1244 cm⁻¹; HRMS calcd for C₂₀H₂₀F₄N₆O₂S₂ [M+1H]⁺: 517.1098; found: 517.1077.



1,2-Bis(2-methyl-5-((E)-(2-thiocarbamoylhydrazone)methyl)furan-3-yl)perfluorocyclobutene (C4F-TSC) (4):

2 (100 mg, 0.29 mmol) and thiosemicarbazide (53 mg, 0.58 mmol) were dissolved in hot EtOH (7 ml) with a few drops of pure acetic acid. The reaction mixture was brought to reflux and stirred for 3 h. After cooling to rt it was poured into water (30 ml) and the precipitate was filtered off. After washing with cold EtOH (3 ml) and drying 13 mg of pale-yellow crystals were obtained. Yield: 91%. m. p. >190°C; ¹H NMR (400 MHz, [D₆]DMSO, 25°C): δ = 2.43 (s, 6H; CH₃), 7.13 (s, 2H; Ar-H (furyl)), 7.76 (br, 2H), 7.93 (s, 2H; HC=N), 8.27 (br, 2H), 11.54 ppm (br, 2H; HNN); ¹³C NMR (100 MHz, [D₆]DMSO, 25°C): δ = 13.61 (CH₃), 110.27 (C-3), 111.55 (CH (furyl)), 118.80 (CF₂ (from ¹⁹F-¹³C-HSQC)), 131.29 (C=N), 149.46 (C-5), 155.97 (C-2), 177.90 ppm (C=S); ¹⁹F NMR (376 MHz, DMSO, 25°C): δ = -109.38 ppm (s); IR: ν = 3257, 3143, 2972, 1582, 1513, 1458 cm⁻¹; HRMS calcd for C₁₈H₁₆F₄N₆O₂S₂ [M+1H]⁺: 489.0785; found: 489.0773.

1. Synthetic Work



1,2-Bis(2-methyl-5-formylthien-3-yl)perfluorocyclobutene (C4F-T-CHO) (5):

4-bromo-5-methyl-2-thienylaldehyde neopentyl acetal^[2] (0.97 g, 3.35 mmol) was dissolved in THF (15 ml). *n*BuLi (2.1 ml, 3.36 mmol, 1.6 M/hexane) was added dropwise at -78°C under N₂ and the reaction mixture was stirred for 30 min at -78°C. A solution of hexafluorocyclobutene (0.3 g, 1.86 mmol) in THF (0.7 ml) was added dropwise and the reaction mixture allowed to warm to rt. After quenching with aqueous NH₄Cl the organic solvent was removed in vacuo, water (50 ml) was added, and the oily residue was extracted with diethyl ether (3x50 ml). The combined organic layers were dried with MgSO₄ and the solvent was removed in vacuo. The oily residue was taken up in acetone (20 ml) and water (10 ml), cooled to 10 °C and conc. HCl (5 ml) was added slowly while maintaining the temperature. The reaction was then stirred at rt. and monitored by TLC. After complete deprotection the organic solvents were removed in vacuo and the residue was brought to pH = 9 by adding aqueous NaHCO₃. After extraction with diethyl ether (3 x 50 ml) the combined organic fractions were dried with MgSO₄ and the solvent was removed in vacuo. The oily residue was purified by column chromatography, thus giving 0.43 g of 7 as brown crystals. Analytically pure 7 was obtained after recrystallization from hexane as yellow crystals. Yield: 69%. R_f = 0.13 (hexanes/EtOAc 2:1); darkens at 90°C with subsequent decomposition; ¹H NMR (600 MHz, CDCl₃, 25°C): δ = 2.57 (s, 6H; CH₃), 7.76 (s, 2H; Ar-H), 9.89 ppm (s, 2H; CHO); ¹³C NMR (150 MHz, CDCl₃, 25°C): δ = 16.01 (CH₃), 118.41 (m, CF₂), 126.49 (C-3), 135.86 (CH (aryl)), 138.86 (m, CCF₂), 142.17 (C-5), 153.13 (C-2), 182.25 ppm (CHO); ¹⁹F NMR (376 MHz, CDCl₃, 25°C): δ = -110.16 ppm (s, 4F); IR: ν = 1654 (C=O), 1537, 1440, 1392 cm⁻¹; MS: *m/z*: 374 [M⁺]; HRMS calcd for C₁₆H₁₀F₄O₂S₂ [M+1H]⁺: 375.0131; found: 375.0098. Closed form isomer of 7: green crystals; ¹H NMR (400 MHz, CDCl₃, 25°C): δ = 2.25 (s, 6H; CH₃), 6.76 (s, 2H; CH (aryl)), 9.85 ppm (s, 2H, CHO); ¹⁹F NMR (376 MHz, CDCl₃, 25°C): δ = -111.11 (m, 2F), -111.32 ppm (m, 2F).

2. UV/vis-Spectra and photochemical kinetics

The UV/vis spectra and photochemical kinetics are represented in Figures S1 – S8. The photochemical quantum yields were determined as described for photoreversible reactions by Gauglitz and coworkers.^[3,4] It is based on the photokinetic equation

$$\frac{dA}{dt} = -I_0 \frac{Cd}{V} F_{pk}^{-1} Q \left\{ A - A_{ps} \right\} \quad (\text{S1})$$

Where A is the absorbance at some probe wavelength, A_{ps} the pertinent value in the photostationary state, I_0 the intensity of the actinic light, C the cross section of the light beam entering the cuvette, d the optical path length, and V the volume of the stirred solution in the cuvette. The photokinetic factor F_{pk} is a function of the absorbance A_{irr} at the irradiation wavelength

$$F_{pk} = \frac{A_{irr}}{1 - 10^{-A_{irr}}} \quad (\text{S2})$$

and the pseudo quantum yield Q is defined as

$$Q = \varepsilon_o \phi_{o \rightarrow c} + \varepsilon_c \phi_{c \rightarrow o} \quad (\text{S3})$$

Here ε_o and ε_c are the molar absorption coefficients of the open and closed form, respectively, of the photo switch and $\phi_{o \rightarrow c}$ and $\phi_{c \rightarrow o}$ the quantum yields for the pertinent photochemical conversions. For irradiation wavelengths 313 and 438 nm, the light intensity I_0 was determined by the azobenzene actinometry procedure described by Gauglitz,^[3,4] for 576 nm by actinometry with mesodiphenyl helianthrene as described by Brauer et al.^[5] Equation S1 is integrated by the procedure given by Gauglitz^[3] and from a fit of the photokinetic data, the pseudo quantum yield Q is determined.

In order to separate the two quantum yields of forward and backward reaction in the pseudo quantum yield, independent information on the composition, viz. the concentrations $c_{o,ps}$ and $c_{c,ps}$ in the photostationary state is required. Their ratio was estimated from NMR spectra of CDCl_3 solutions irradiated to a saturation of the ratio of the two forms. Since these experiments were performed with a higher concentration than in the photokinetic experiment and in a deuterated solvent, the open/closed ratio from the NMR experiment may differ somewhat from that reached in the photokinetic experiment. Therefore, estimates of the open/closed ratio in the photostationary state were also based on other criteria such as the assumption of independence of $\phi_{c \rightarrow o}$ on the irradiation wavelength (according to the Kasha rule) and the requirement that the spectrum of the pure closed form, extrapolated from the photostationary state spectrum should never fall below the zero line.

Based on the values of $c_{o,ps}$ and $c_{c,ps}$ in the photostationary state, the individual quantum yields of forward and backward reaction are obtained by the equations

$$\phi_{o \rightarrow c} = \frac{Q}{\varepsilon_o (1 + c_{o,ps} / c_{c,ps})} \quad (\text{S4})$$

$$\text{and } \phi_{c \rightarrow o} = \frac{Q - \varepsilon_o \phi_{o \rightarrow c}}{\varepsilon_c} \quad (\text{S5})$$

The absorption coefficient ε_c of the closed form, required in equation S5 can be extrapolated from the absorption coefficient ε_{ps} of the photostationary mixture by

$$\varepsilon_c = \varepsilon_o + (\varepsilon_{ps} - \varepsilon_o) c / c_{c,ps} \quad (\text{S6})$$

2. UV-vis-Spectra and photochemical kinetics

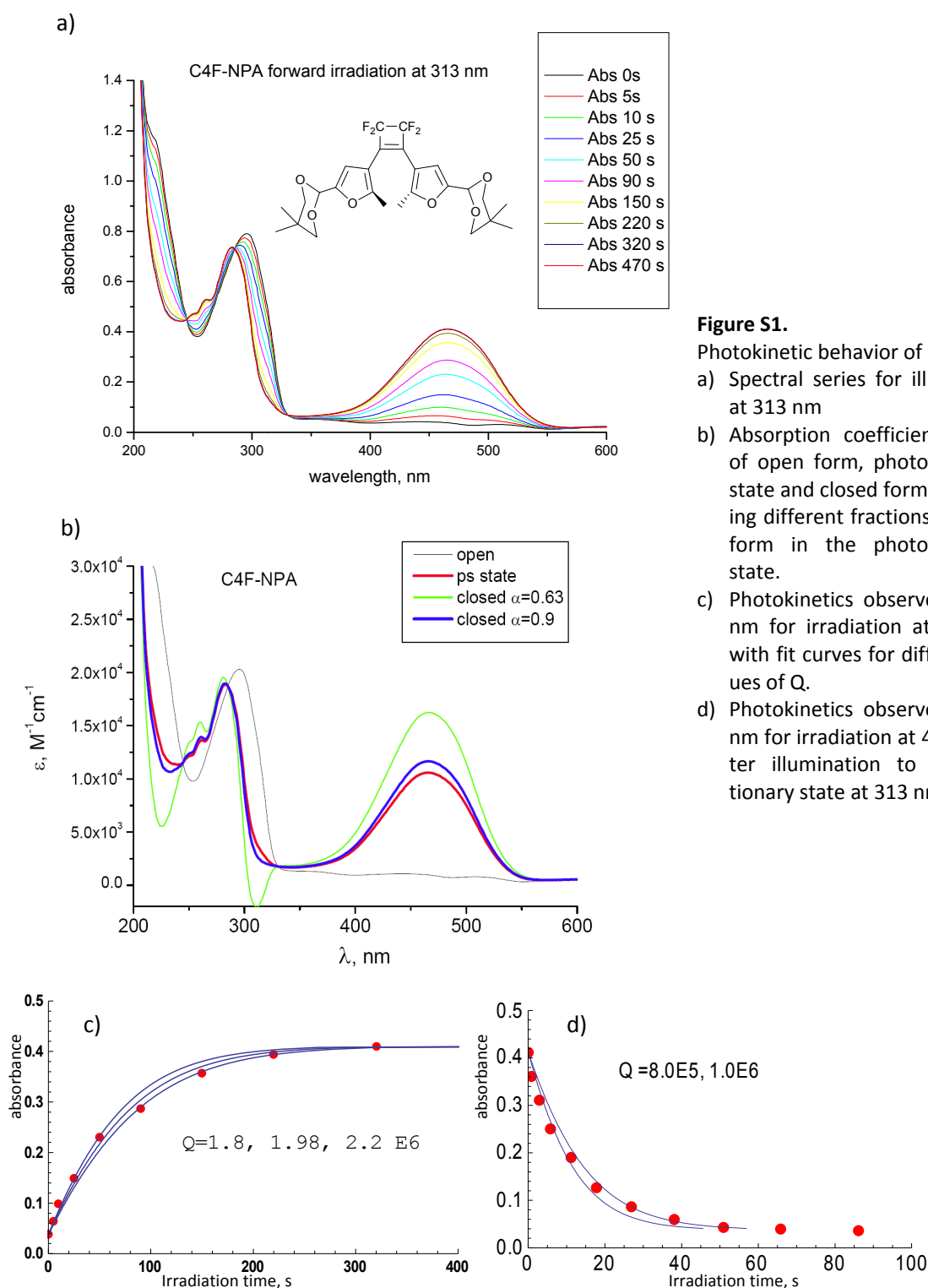


Figure S1.

- a) Spectral series for illumination at 313 nm
- b) Absorption coefficient spectra of open form, photostationary state and closed form assuming different fractions of closed form in the photostationary state.
- c) Photokinetics observed at 466 nm for irradiation at 313 nm, with fit curves for different values of Q .
- d) Photokinetics observed at 472 nm for irradiation at 438 nm after illumination to photostationary state at 313 nm.

Summary of data for C4F-NPA

Solvent: CHCl_3

Irradiation at 313 nm: $I_0 = 1.32 \times 10^{-8} \text{ E s}^{-1} \text{ cm}^{-2}$, $Q = 1.98 \times 10^6 \text{ cm}^2 \text{ mol}^{-1}$

Irradiation at 438 nm: $I_0 = 1.49 \times 10^{-7} \text{ E s}^{-1} \text{ cm}^{-2}$, $Q = 8.03 \times 10^5 \text{ cm}^2 \text{ mol}^{-1}$

Closed-fraction in photostationary state and quantum yields

63% (NMR): $\Phi_{o \rightarrow c}(313) = 9.7\%$ $\Phi_{c \rightarrow o}(313) = -38\%$ $\Phi_{c \rightarrow o}(438) = 6.1\%$

89% (*): $\Phi_{o \rightarrow c}(313) = 14\%$ $\Phi_{c \rightarrow o}(313) = 8.6\%$ $\Phi_{c \rightarrow o}(438) = 8.6\%$

(*) yields λ -indep. $\Phi_{o \rightarrow c}$ and reasonable absorption spectrum of closed form, cf. Fig. b)

2. UV-vis-Spectra and photochemical kinetics

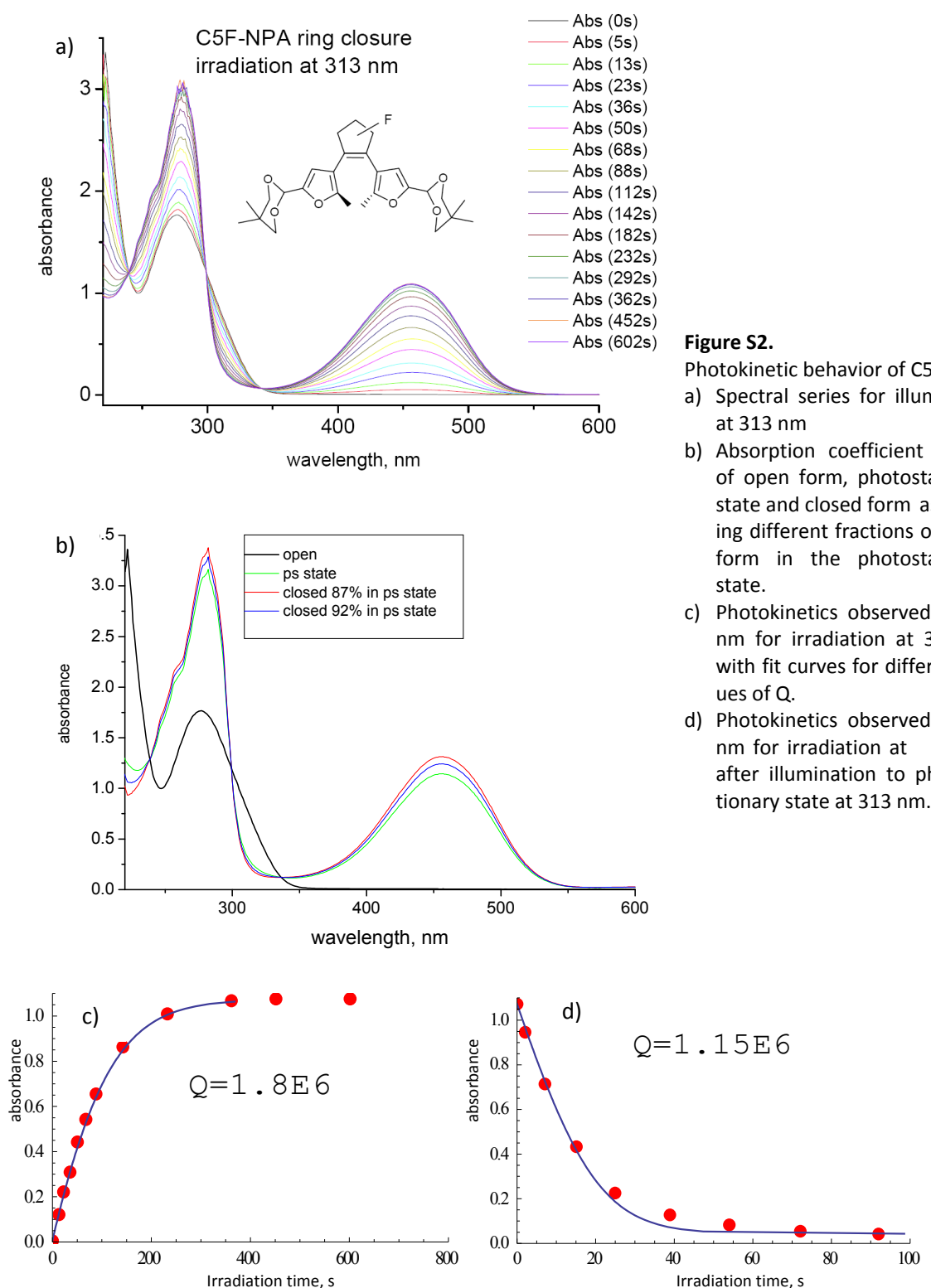


Figure S2.

- a) Spectral series for illumination at 313 nm
- b) Absorption coefficient spectra of open form, photostationary state and closed form assuming different fractions of closed form in the photostationary state.
- c) Photokinetics observed at 450 nm for irradiation at 313 nm, with fit curves for different values of Q .
- d) Photokinetics observed at 470 nm for irradiation at 438 nm after illumination to photostationary state at 313 nm.

Summary of data for C5F-NPA

Solvent: CHCl_3

Irradiation at 313 nm: $I_0 = 1.32 \times 10^{-8} \text{ E s}^{-1} \text{ cm}^{-2}$, $Q = 1.80 \times 10^6 \text{ cm}^2 \text{ mol}^{-1}$

Irradiation at 438 nm: $I_0 = 1.49 \times 10^{-7} \text{ E s}^{-1} \text{ cm}^{-2}$, $Q = 1.15 \times 10^6 \text{ cm}^2 \text{ mol}^{-1}$

Closed-fraction in photostationary state and quantum yields

87% (NMR): $\Phi_{o \rightarrow c}(313) = 19\%$ $\Phi_{c \rightarrow o}(313) = 13\%$ $\Phi_{c \rightarrow o}(438) = 8.6\%$

92% (*): $\Phi_{o \rightarrow c}(313) = 20\%$ $\Phi_{c \rightarrow o}(313) = 9.0\%$ $\Phi_{c \rightarrow o}(438) = 9.0\%$

(*) yields λ -indep. $\Phi_{o \rightarrow c}$ and reasonable absorption spectrum of closed form, cf. Fig. b)

2. UV-vis-Spectra and photochemical kinetics

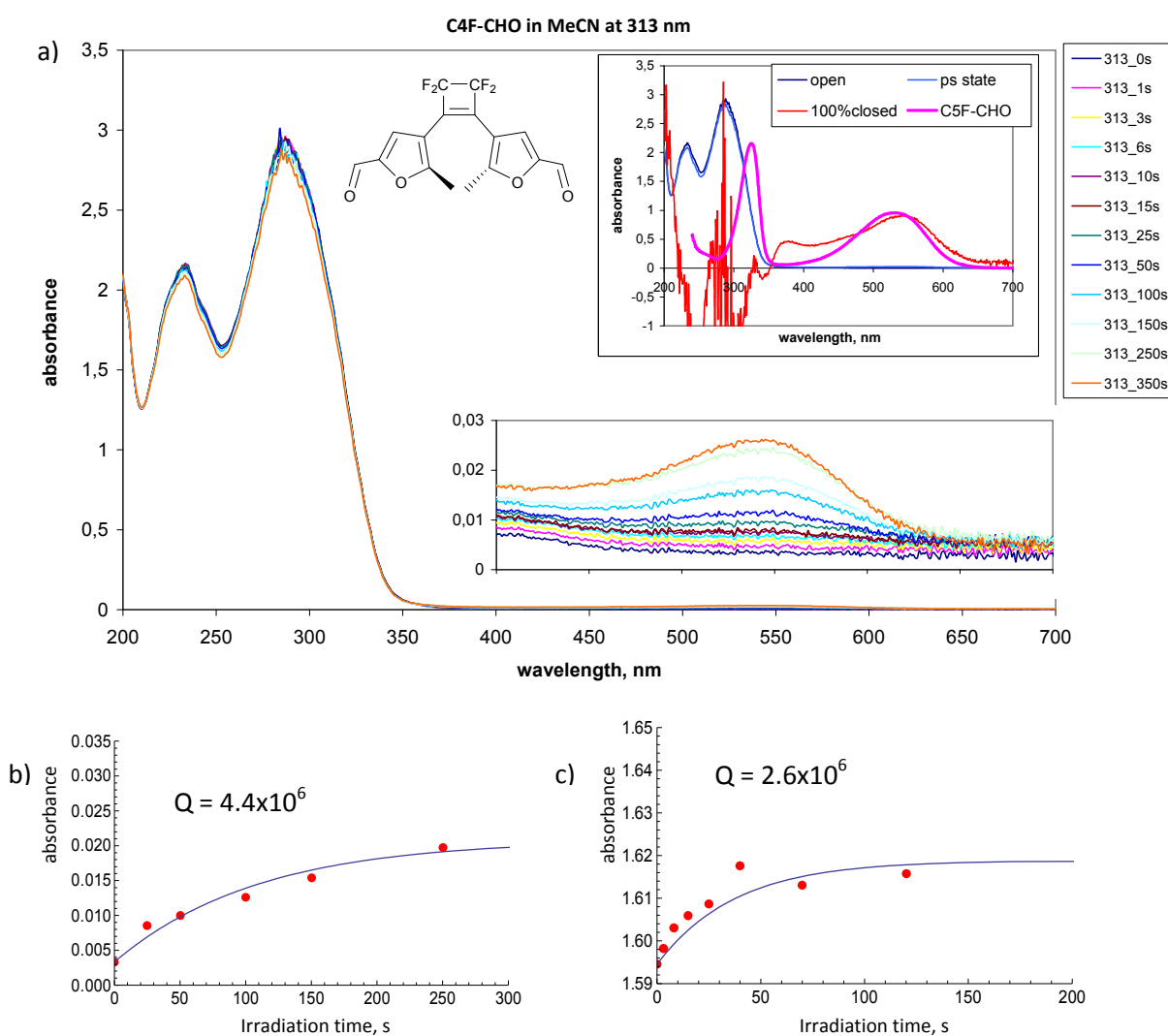


Figure S3. Experimental results for irradiation of **C4F-CHO** 1.14×10^{-4} M in MeCN.

a) Spectral series recorded during illumination at 313 nm. Lower inset: enlarged scale in the long wavelength region. Upper inset: extrapolated spectrum of 100% closed form assuming 2.5% closed in the photostationary state in comparison to pure closed spectrum of C5F-CHO. The noisy section of the 100% closed spectrum around 300 results from the difference of two large absorbances of pure open form and ps-state spectrum. The concentration had to be chosen very high, in order to resolve the weak absorbance of the ps-state in the visible.

b) photokinetic curve for illumination at 313 nm and observation at 401 nm.

c) photokinetic curve for illumination at 576 nm and observation at 251 nm.

Summary of data for C4F-CHO

solvent: acetonitrile

Irradiation at 313 nm: $I_0 = 1.18 \times 10^{-8} \text{ E s}^{-1} \text{ cm}^{-2}$, $Q = 4.4 \times 10^6 \text{ cm}^2 \text{ mol}^{-1}$

Irradiation at 576 nm: $I_0 = 1.37 \times 10^{-8} \text{ E s}^{-1} \text{ cm}^{-2}$, $Q = 2.6 \times 10^6 \text{ cm}^2 \text{ mol}^{-1}$

Closed fraction in photostationary state and quantum yields

2.5%* $\Phi_{o \rightarrow c}(313) = 1.0\%$ $\Phi_{c \rightarrow o}(313) = 27\%$ $\Phi_{c \rightarrow o}(576) = 46\%$

*with this value, the extrapolated spectrum in the visible for 100% closed form approximately matches the spectrum of the closed form of C5F-CHO. The latter is a reasonable standard because in all other cases investigated in this paper the spectra of the C4F and corresponding C5F compounds were very similar.

2. UV-vis-Spectra and photochemical kinetics

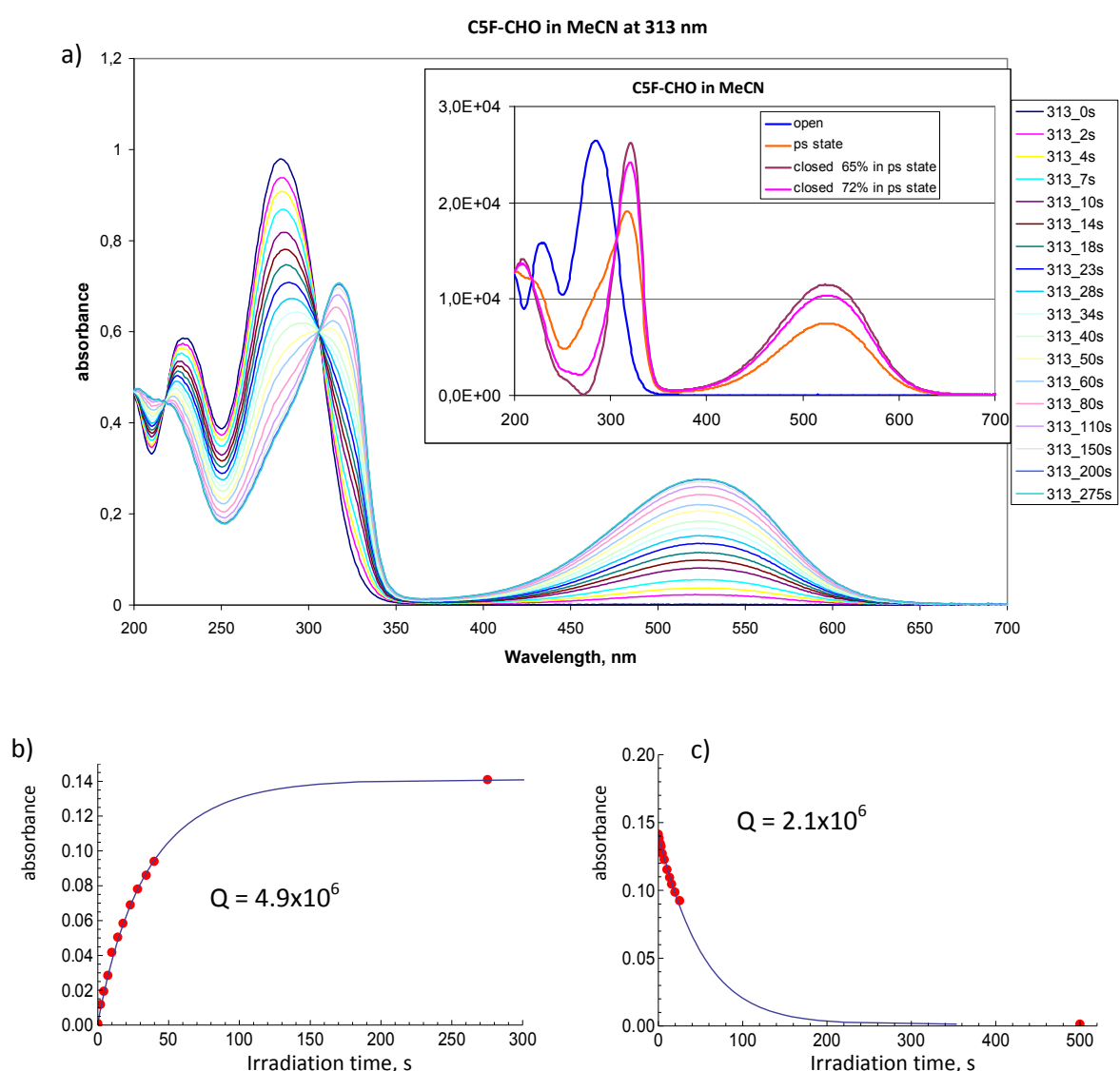
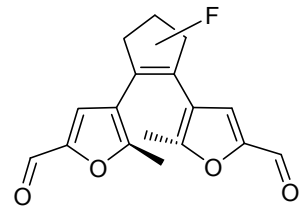


Figure S4. Photokinetic behavior of C5F-CHO.

- Spectral series for illumination at 313 nm. Inset: absorption coefficient spectra of open form, photostationary state and closed form assuming different fractions of closed form in the photostationary state.
- Photokinetics observed at 576 nm for irradiation at 313 nm, with fit curve for given value of Q .
- Photokinetics observed at 576 nm for irradiation at 576 nm after illumination to photostationary state at 313, with fit curve for given value of Q .



Summary of data for C5F-CHO

Solvent: acetonitrile

Irradiation at 313 nm: $I_0 = 1.27 \times 10^{-8} \text{ E s}^{-1} \text{ cm}^{-2}$, $Q = 4.90 \times 10^6 \text{ cm}^2 \text{ mol}^{-1}$

Irradiation at 576 nm: $I_0 = 1.32 \times 10^{-8} \text{ E s}^{-1} \text{ cm}^{-2}$, $Q = 8.03 \times 10^5 \text{ cm}^2 \text{ mol}^{-1}$

Closed-fraction in photostationary state and quantum yields

72% (from NMR in CDCl_3): $\Phi_{o \rightarrow c}(313) = 34\%$ $\Phi_{c \rightarrow o}(313) = 6.3\%$ $\Phi_{c \rightarrow o}(576) = 15\%$

65% (for comparison)*: $\Phi_{o \rightarrow c}(313) = 31\%$ $\Phi_{c \rightarrow o}(313) = 7.4\%$ $\Phi_{c \rightarrow o}(576) = 14\%$

*The 72% case yields the more reasonable spectrum of the closed form in the UV region around 280 nm. Only for 44% closed form in the ps state one would obtain equal quantum yields for ring opening at 313 and 576 nm. For such a composition, however, the absorption of the pure closed form would turn out to be extremely negative below 300 nm.

2. UV-vis-Spectra and photochemical kinetics

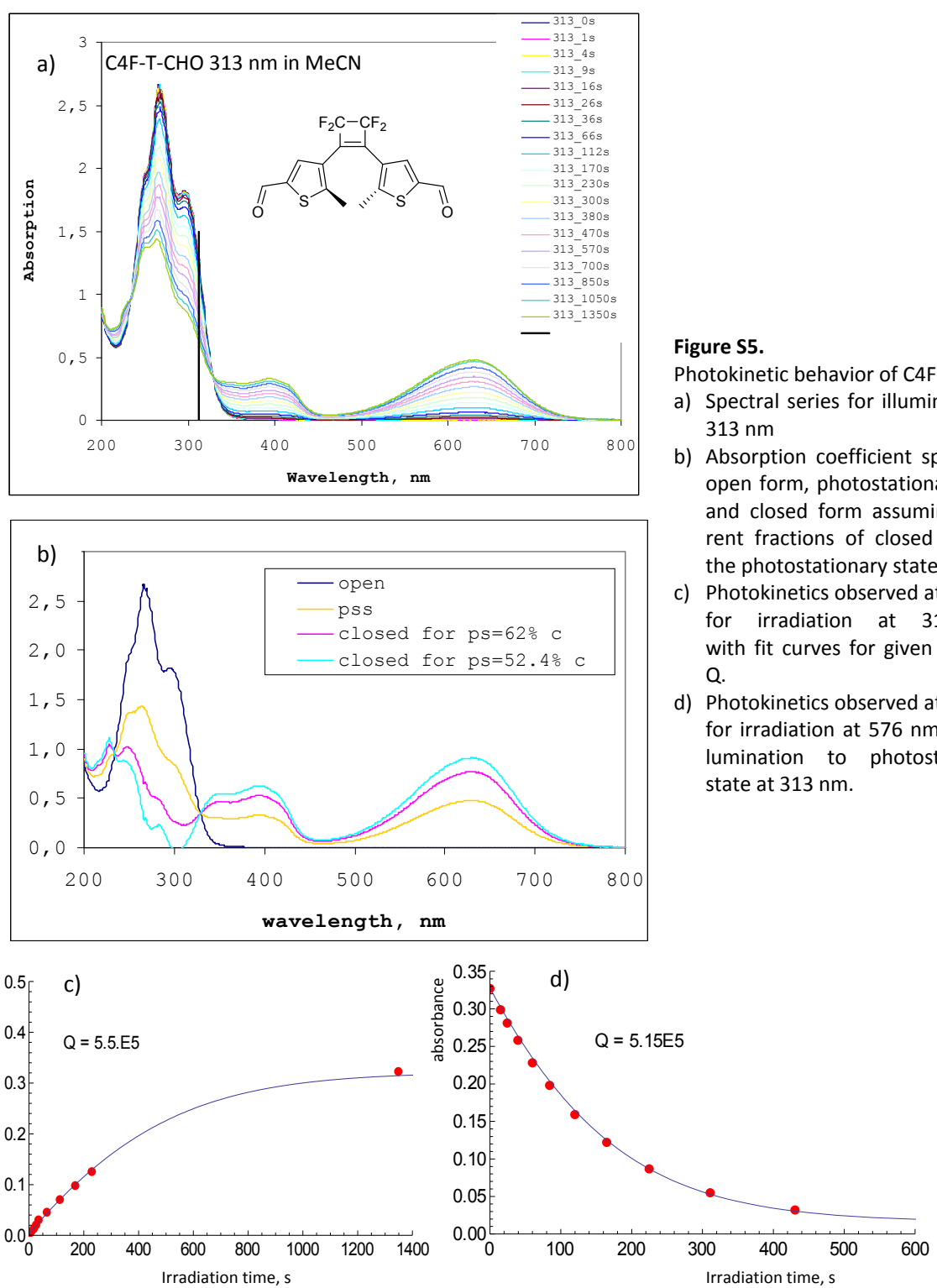


Figure S5.

- Photokinetic behavior of C₄F-T-CHO
- Spectral series for illumination at 313 nm
 - Absorption coefficient spectra of open form, photostationary state and closed form assuming different fractions of closed form in the photostationary state.
 - Photokinetics observed at 401 nm for irradiation at 313 nm, with fit curves for given value of Q.
 - Photokinetics observed at 390 nm for irradiation at 576 nm after illumination to photostationary state at 313 nm.

Summary of data for C₄F-T-CHO

Solvent: CH₃CN

Irradiation at 313 nm: $I_0 = 1.43 \times 10^{-8} \text{ E s}^{-1} \text{ cm}^{-2}$, $Q = 5.53 \times 10^5 \text{ cm}^2 \text{ mol}^{-1}$

Irradiation at 576 nm: $I_0 = 2.03 \times 10^{-8} \text{ E s}^{-1} \text{ cm}^{-2}$, $Q = 5.16 \times 10^5 \text{ cm}^2 \text{ mol}^{-1}$

Closed-fraction in photostationary state and quantum yields

52% (NMR):	$\Phi_{o \rightarrow c}(313) = 2.2\%$	$\Phi_{c \rightarrow o}(313) = 56\%$	$\Phi_{c \rightarrow o}(576) = 7.4\%$
62% (*):	$\Phi_{o \rightarrow c}(313) = 2.6\%$	$\Phi_{c \rightarrow o}(313) = 8.8\%$	$\Phi_{c \rightarrow o}(576) = 8.8\%$

(*) yields λ -indep. $\Phi_{o \rightarrow c}$ and reasonable absorption spectrum of closed form, cf. Fig. b)

2. UV-vis-Spectra and photochemical kinetics

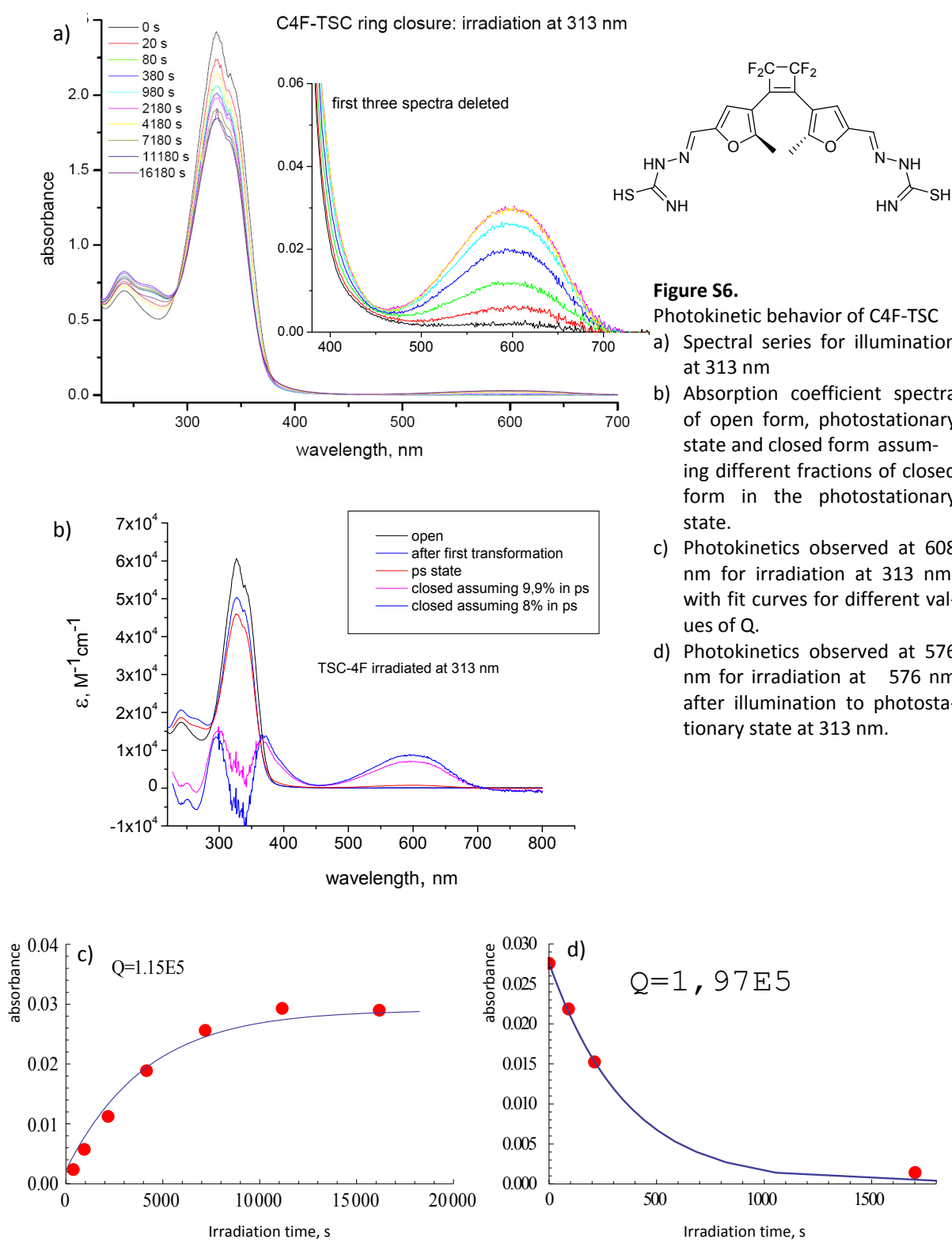


Figure S6.

- Photokinetic behavior of C4F-TSC
- a) Spectral series for illumination at 313 nm
 - b) Absorption coefficient spectra of open form, photostationary state and closed form assuming different fractions of closed form in the photostationary state.
 - c) Photokinetics observed at 608 nm for irradiation at 313 nm, with fit curves for different values of Q.
 - d) Photokinetics observed at 576 nm for irradiation at 576 nm after illumination to photostationary state at 313 nm.

Summary of data for C4F-TSC

Solvent: CHCl_3

Irradiation at 313 nm: $I_0 = 1.02 \times 10^{-8} \text{ E s}^{-1} \text{ cm}^{-2}$, $Q = 1.15 \times 10^5 \text{ cm}^2 \text{ mol}^{-1}$

Irradiation at 576 nm: $I_0 = 1.89 \times 10^{-8} \text{ E s}^{-1} \text{ cm}^{-2}$, $Q = 1.97 \times 10^5 \text{ cm}^2 \text{ mol}^{-1}$

Closed-fraction in photostationary state and quantum yields

8.0% (NMR): $\Phi_{o \rightarrow c}(313) = 0.029\%$ $\Phi_{c \rightarrow o}(313) = 1.0\%$

9.9% (*): $\Phi_{o \rightarrow c}(313) = 0.024\%$ $\Phi_{c \rightarrow o}(313) = 2.5\%$

(*) yields λ -indep. $\Phi_{o \rightarrow c}$ and reasonable absorption spectrum of closed form, cf. Fig. b)

$\Phi_{c \rightarrow o}(576) = 2.8\%$

$\Phi_{c \rightarrow o}(576) = 2.4\%$

2. UV-vis-Spectra and photochemical kinetics

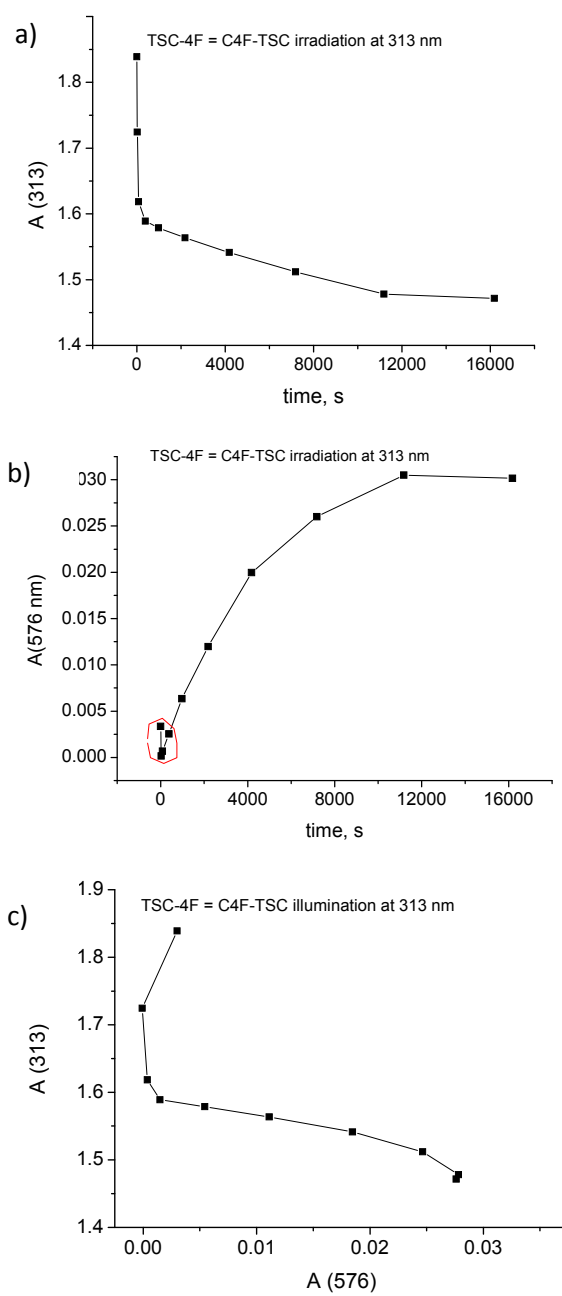


Figure S7. C4F-TSC: Correlation of spectral changes for irradiation at 313 nm.

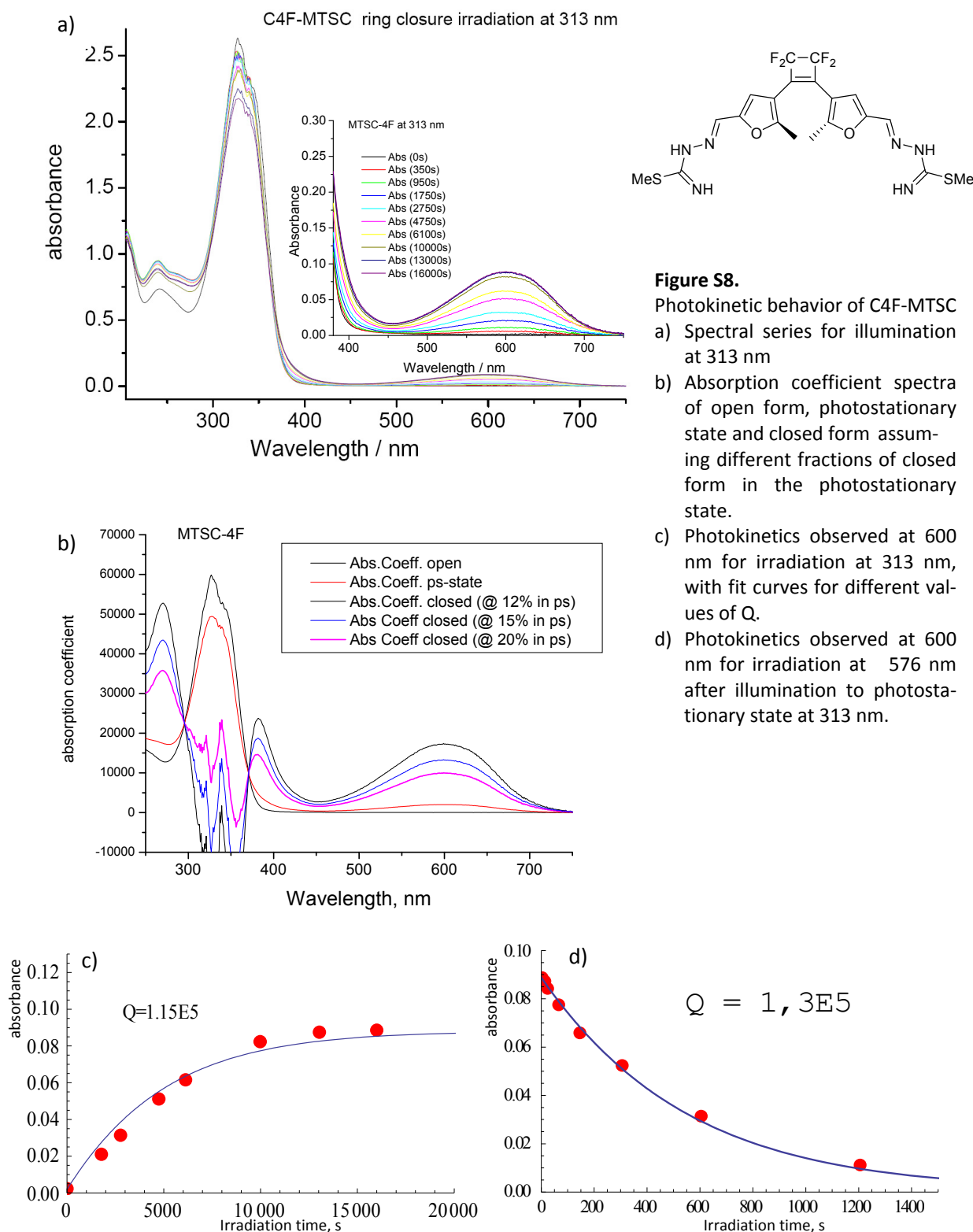
a) A (313) versus time.

b) A (576) versus time.

c) A (313) versus A(576)

The diagrams show that within the first 300 s there is little change in the long wavelength band, but a considerable decrease in the short wavelength band. On the other hand the change in absorbance at 313 nm is only moderate during the period of largest change at the long wavelength maximum. These observations indicate that the photo process is not uniform. Ring closure is not the first photo process but seems to require another photo transformation of the starting compound beforehand.

2. UV-vis-Spectra and photochemical kinetics



Summary of data for C4F-MTSC

Solvent: CHCl_3

Irradiation at 313 nm: $I_0 = 1.03 \times 10^{-8} \text{ E s}^{-1} \text{ cm}^{-2}$, $Q = 1.15 \times 10^5 \text{ cm}^2 \text{ mol}^{-1}$

Irradiation at 576 nm: $I_0 = 1.98 \times 10^{-8} \text{ E s}^{-1} \text{ cm}^{-2}$, $Q = 1.3 \times 10^5 \text{ cm}^2 \text{ mol}^{-1}$

Closed-fraction in photostationary state and quantum yields

12% (NMR): $\Phi_{o \rightarrow c}(313) = 0.029\%$ $\Phi_{c \rightarrow o}(313) = -3.4\%$ $\Phi_{c \rightarrow o}(576) = 0.79\%$

15% (*): $\Phi_{o \rightarrow c}(313) = 0.039\%$ $\Phi_{c \rightarrow o}(313) = 1.1\%$ $\Phi_{c \rightarrow o}(576) = 1.0\%$

(*) yields λ -indep. $\Phi_{o \rightarrow c}$ and reasonable absorption spectrum of closed form, cf. Fig. b)

2. UV/vis-Spectra and photochemical kinetics

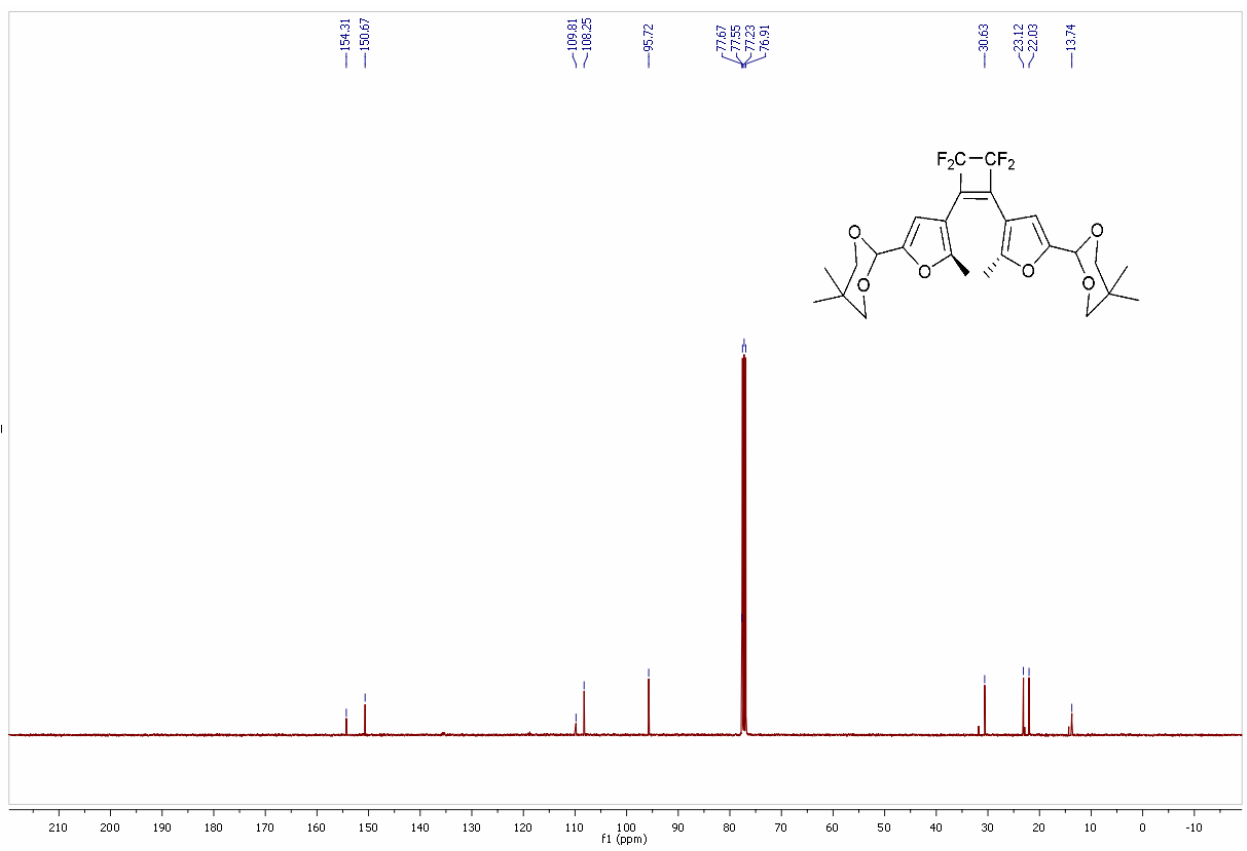
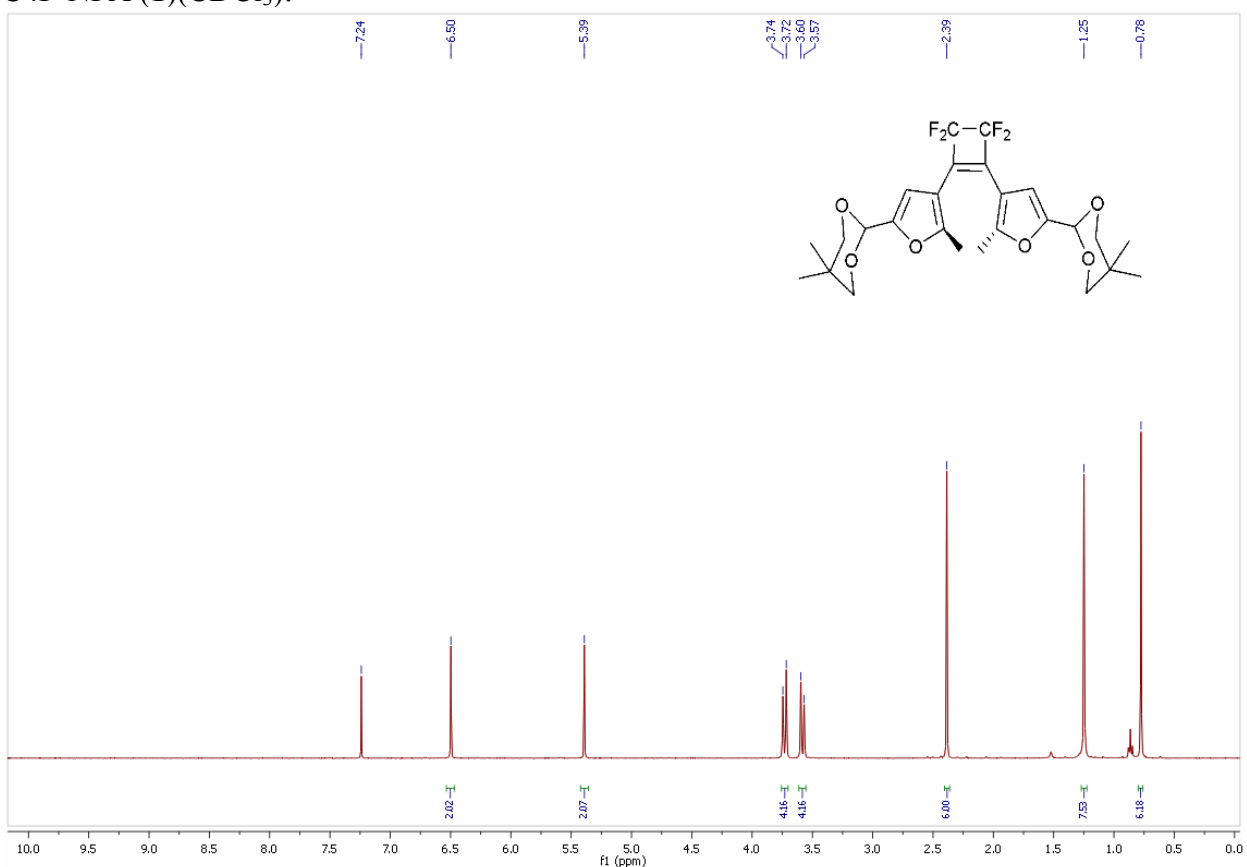
Table S1 Wavelengths and molar absorption coefficients of first absorption maxima^a

π -substituent	C4F-open		C5F-open		C4F- closed		C5F-closed	
	λ_{\max} [nm]	ε [$M^{-1}cm^{-1}$]						
NPA	295	$2,0 \times 10^4$	277	$2,0 \times 10^4$	466	$1,2 \times 10^4$	458	$1,5 \times 10^4$
CHO	288 ^[b]	$2,6 \times 10^4$	289 ^[b]	$2,6 \times 10^4$	544 ^[b]	$8,0 \times 10^3$	533 ^[b]	$1,0 \times 10^4$
T-CHO	265 ^[b]	$2,9 \times 10^4$	264 ^[c]	$3,9 \times 10^4$	627 ^[b]	$8,2 \times 10^3$	618 ^[c]	$8,8 \times 10^3$
TSC	327	$6,1 \times 10^4$	327 ^[d]	$5,5 \times 10^4$	595	$7,1 \times 10^3$	576 ^[d]	$1,5 \times 10^4$
MTSC	327	$6,0 \times 10^4$	329 ^[d]	$6,0 \times 10^4$	592	$1,3 \times 10^4$	575 ^[d]	$1,8 \times 10^4$

^a solvent CHCl₃ unless given otherwise; ^b solvent CH₃CN; ^c solvent CH₂Cl₂, data from ref. [6]; ^d solvent MeOH, data from ref. [7].

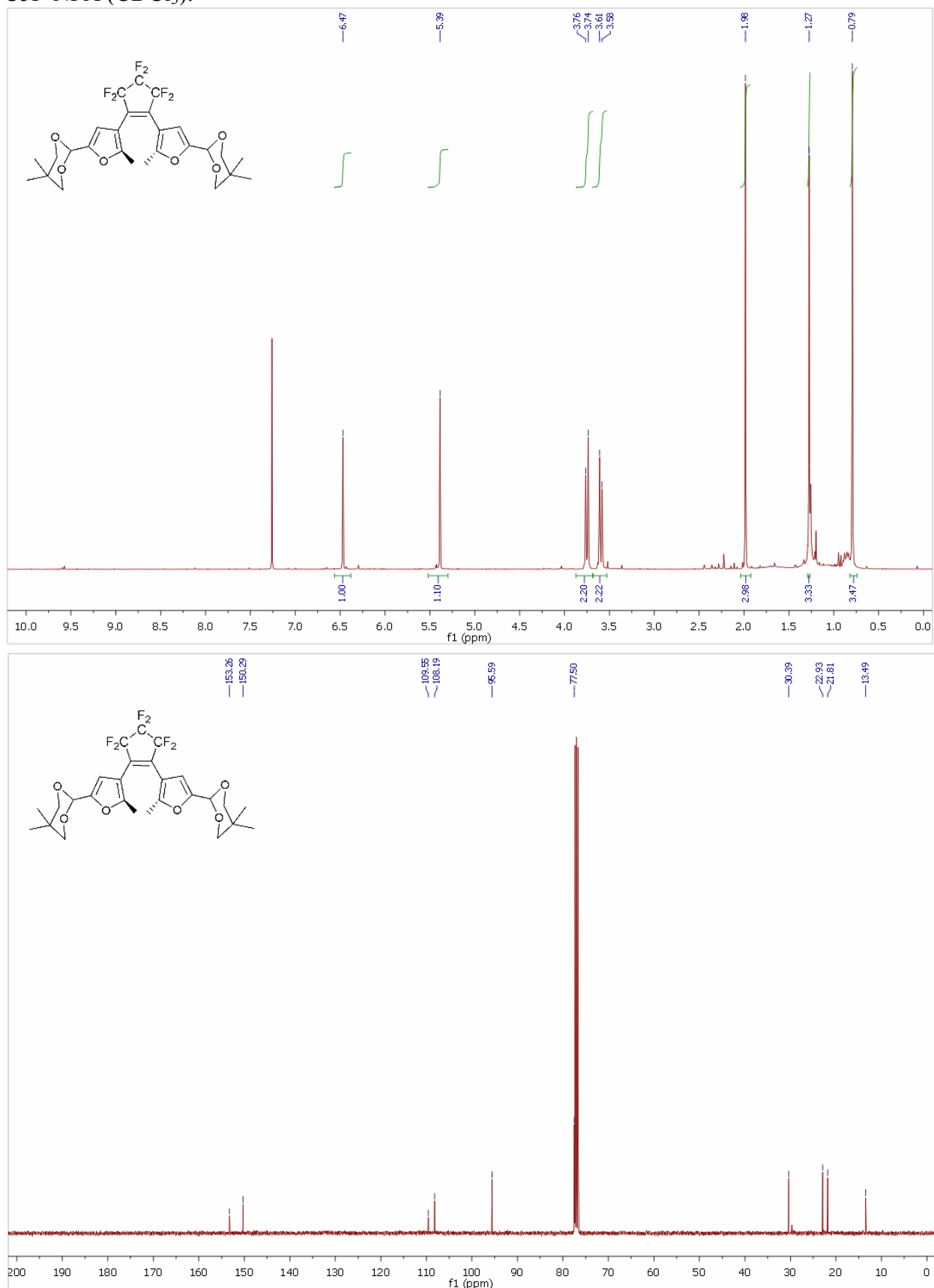
3. NMR-Spectra

C4F-NPA (**1**)(CDCl₃):



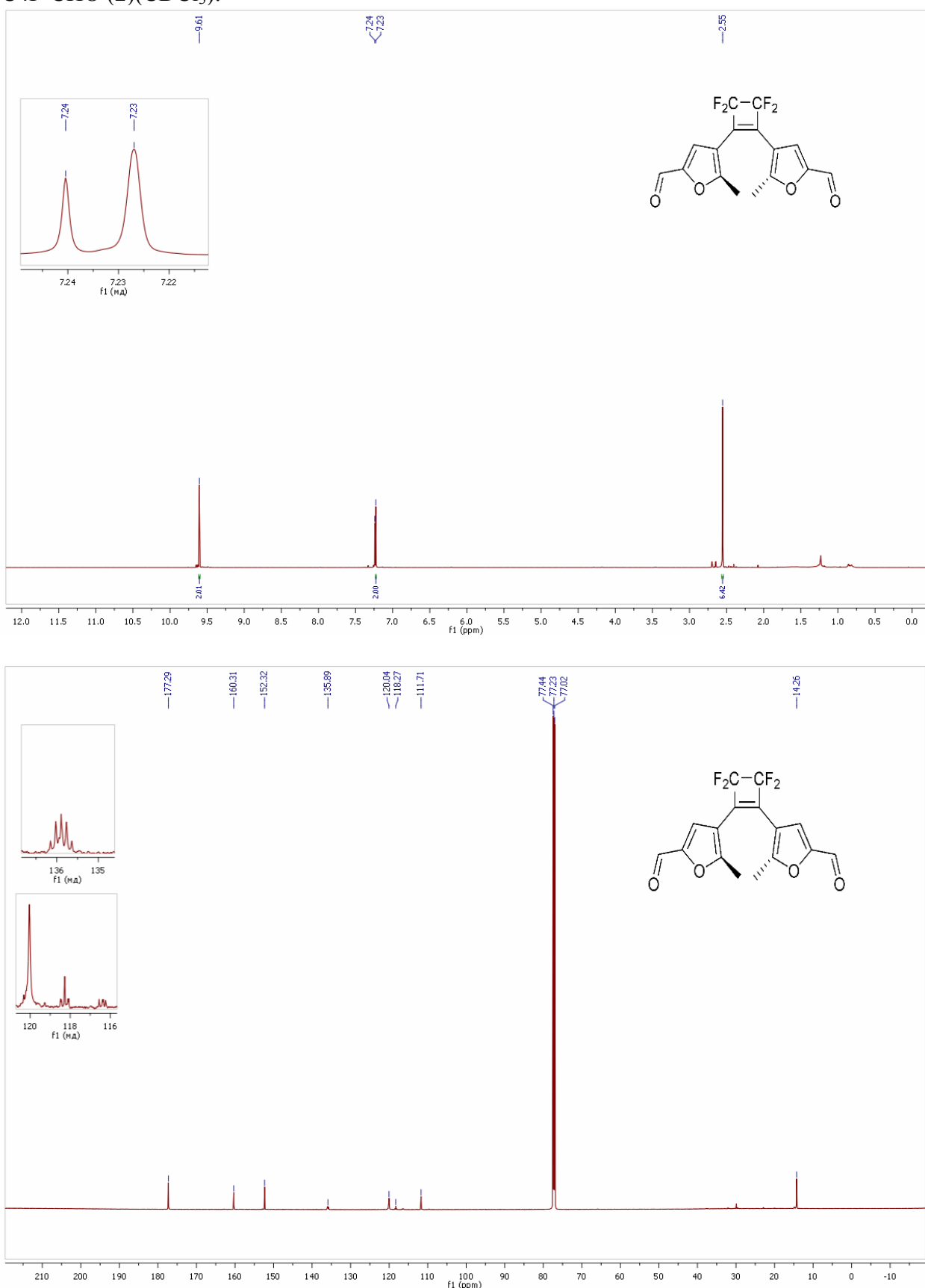
3. NMR-Spectra

C5F-NPA (CDCl_3):



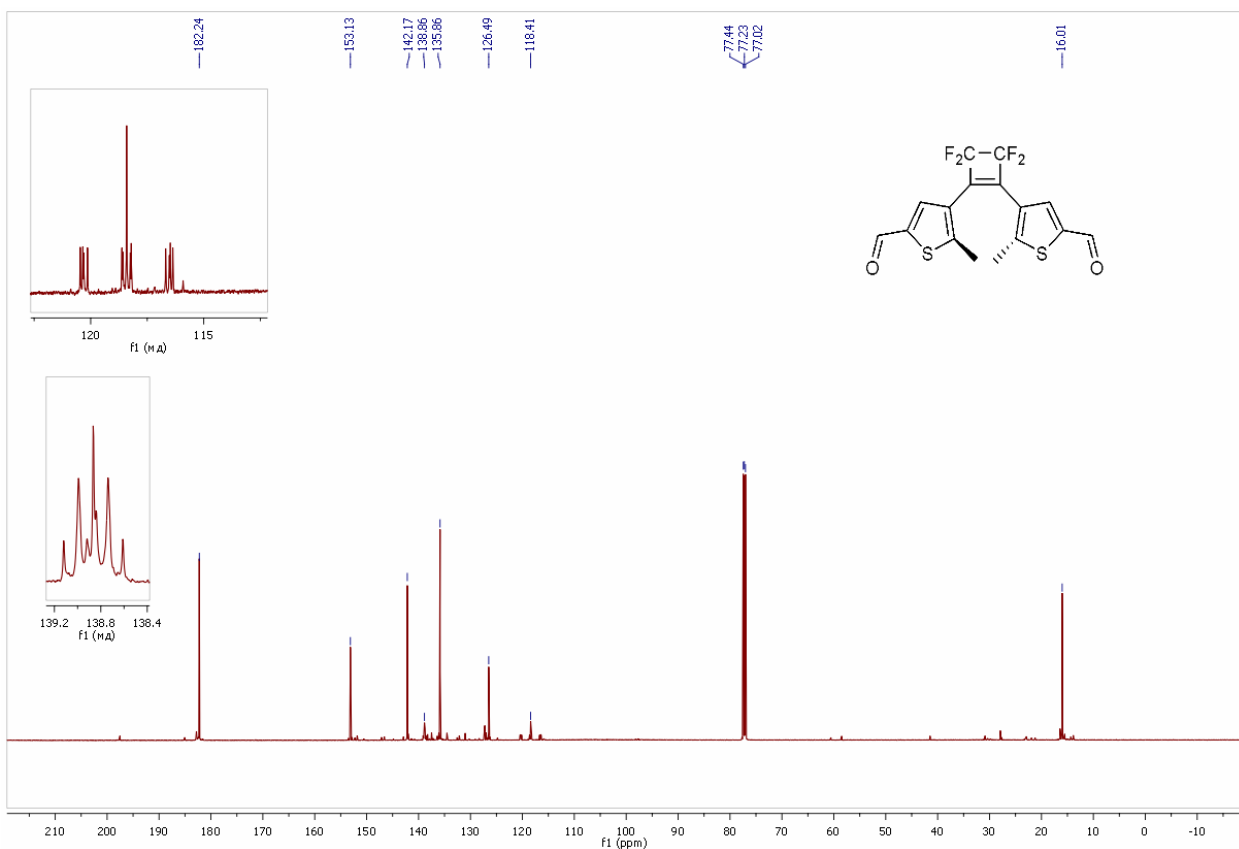
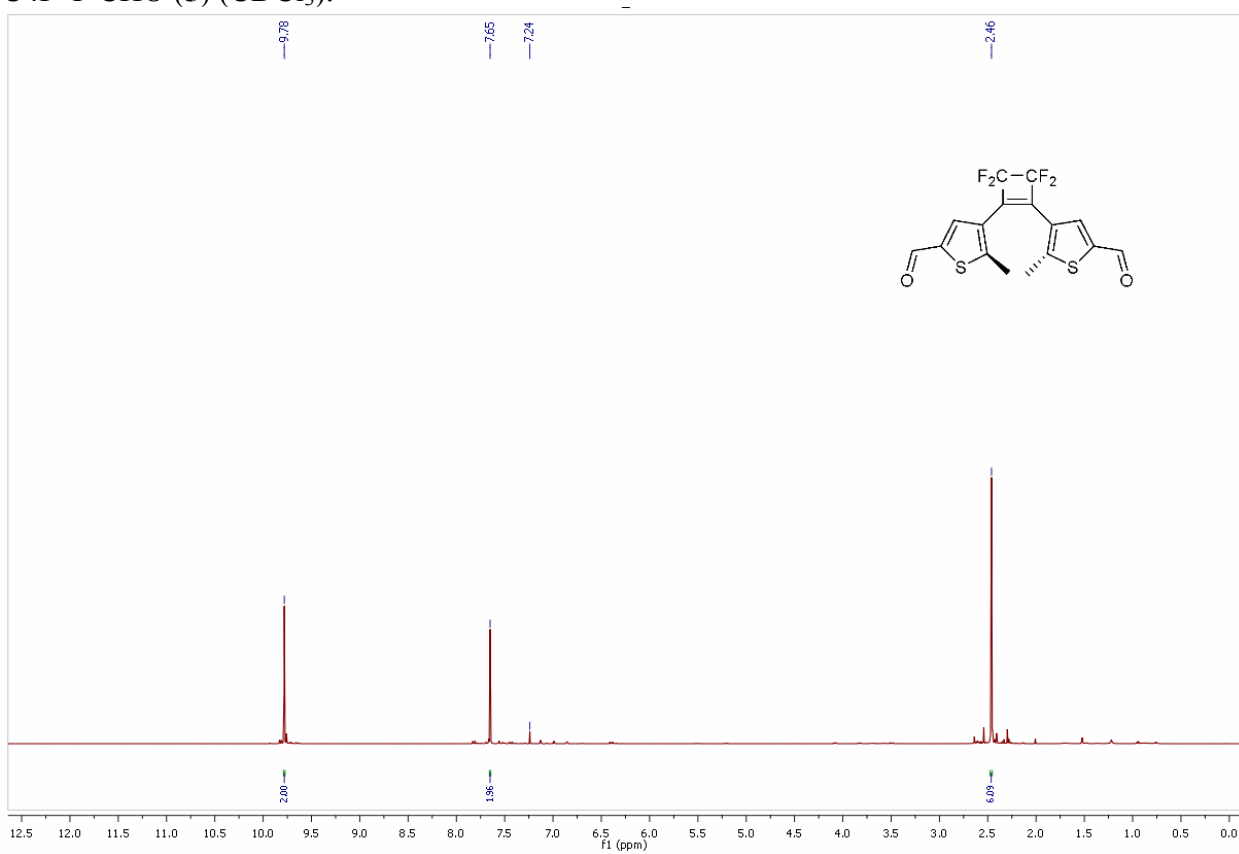
3. NMR-Spectra

C4F-CHO (**2**)(CDCl₃):



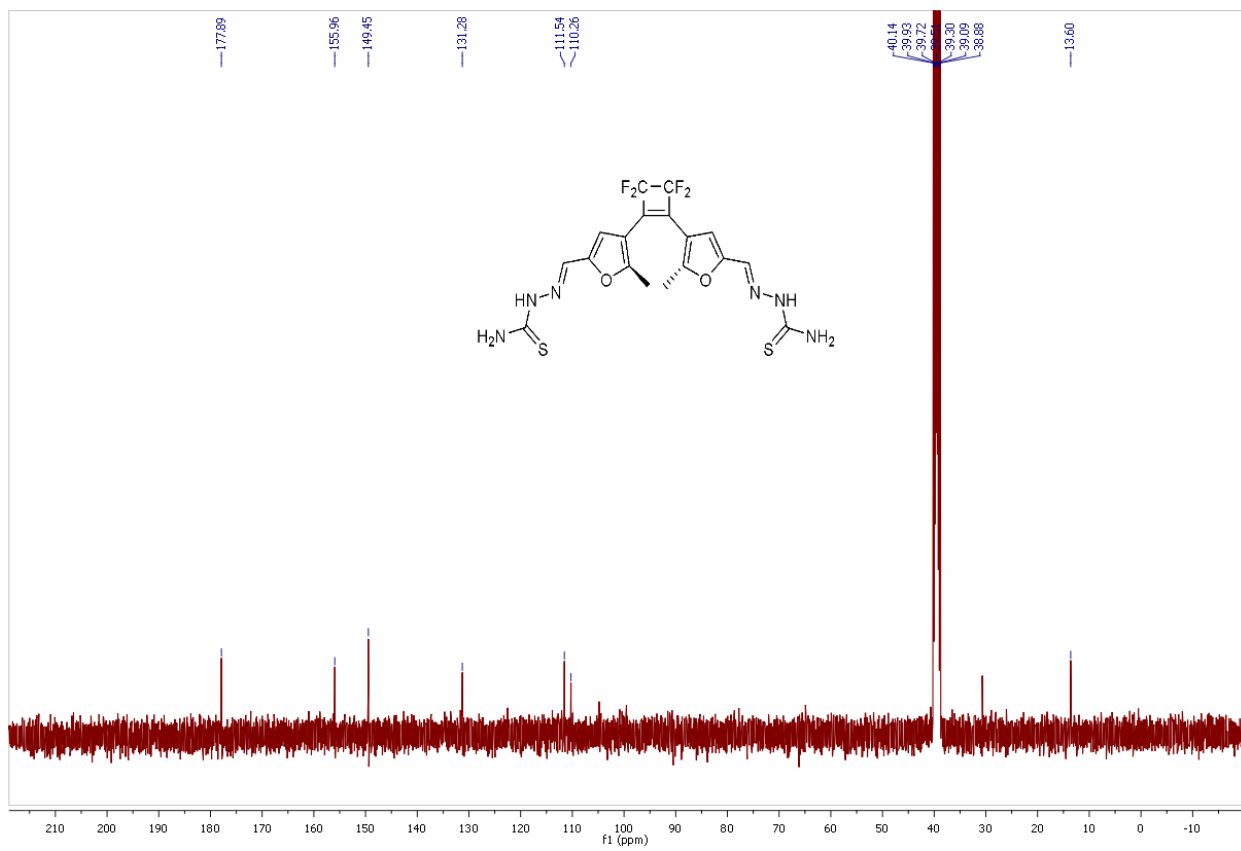
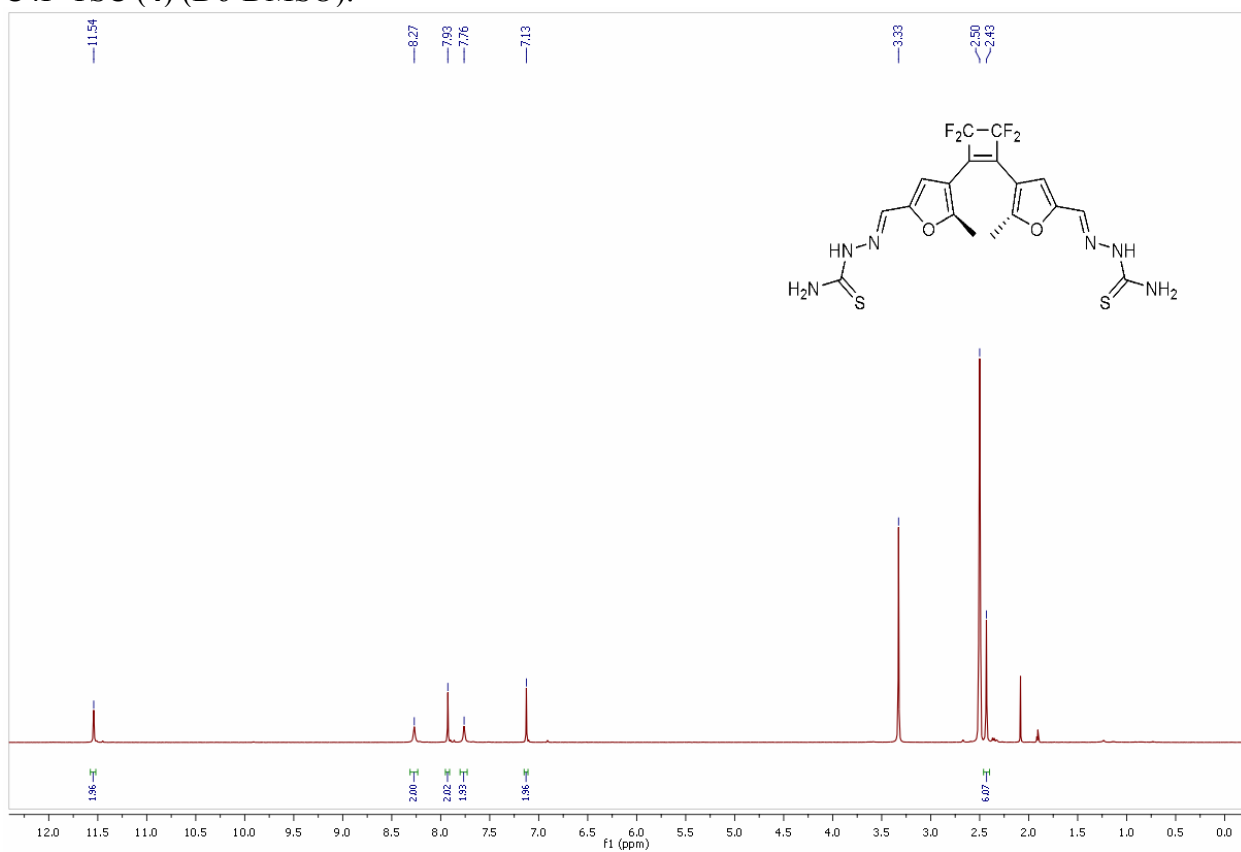
3. NMR-Spectra

C4F-T-CHO (**5**) (CDCl_3):



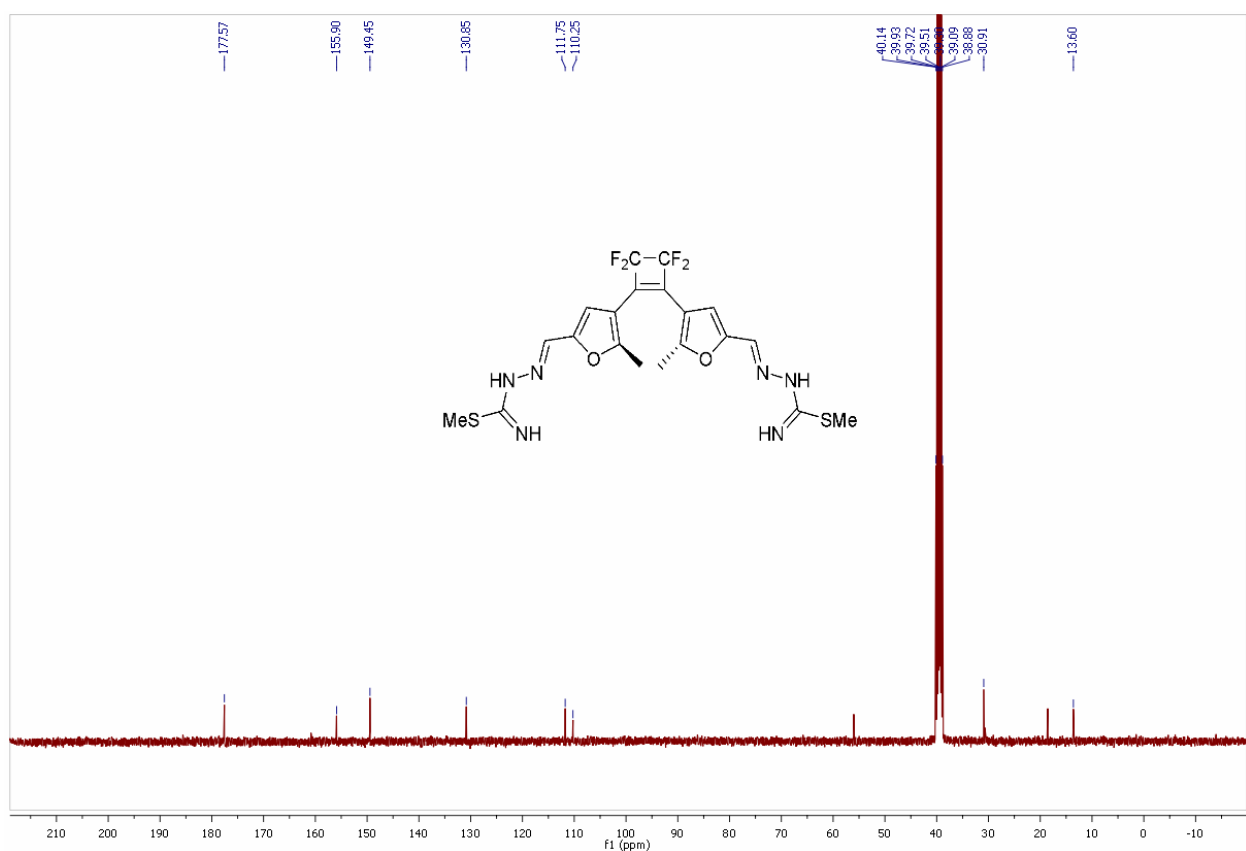
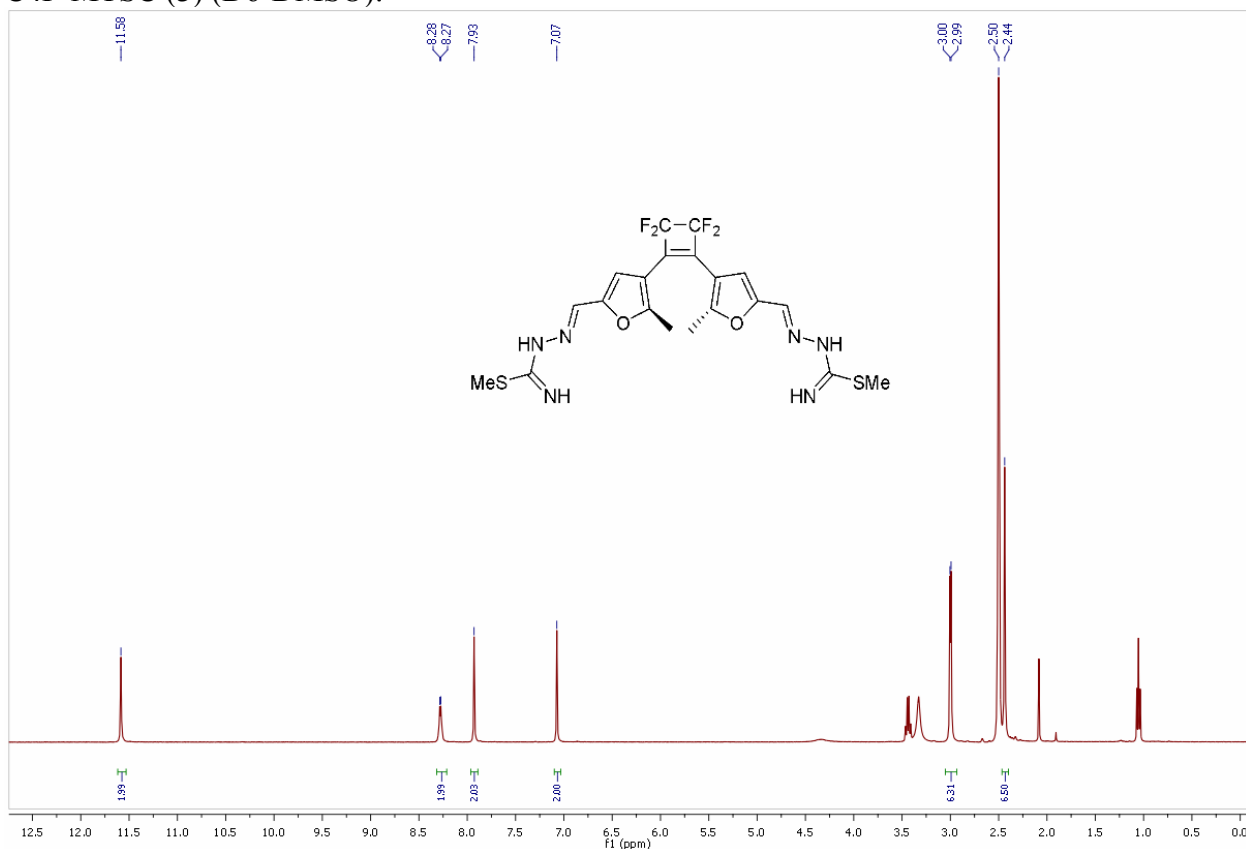
3. NMR-Spectra

C4F-TSC (**4**) (D6-DMSO):



3. NMR-Spectra

C4F-MTSC (**3**) (D6-DMSO):



4. Crystallographic Data

Materials and Methods

Data collection for X-ray structure-determination was performed at a *STOE IPDS-II* diffractometer equipped with a graphite monochromated radiation source ($\lambda = 0.71073 \text{ \AA}$), an image plate detection system and an *Oxford Cryostream 700* with nitrogen as coolant gas. The selection, integration, and averaging procedure of the measured reflex intensities, the determination of the unit cell by a least-squares fit of the 2Θ values, data reduction, LP correction, and the space group determination were performed using the *X-Area* software package delivered with the diffractometer. A semiempirical absorption correction method was performed after indexing of the crystal faces. The structures were solved by direct methods (*SHELXS-97*)^[8] and refined by standard Fourier techniques against F square with a full-matrix leastsquares algorithm using *SHELXL-97* and the *WinGX* (1.80.05)^[9] software package. All non-hydrogen atoms were refined anisotropically. Hydrogen atoms were placed in calculated positions and refined with a riding model. Graphical representations were prepared with *ORTEP-III*.^[10] Crystallographic data (excluding structure factors) of **1**, **2** and **5** have been deposited with the Cambridge Crystallographic Data Centre as supplementary publication CCDC 832576, 856183 and 832577, respectively. Copies of the data can be obtained free of charge on application to CCDC, 12 Union Road, Cambridge CB21EZ, U.K. (fax: (+44)1223–336–033. e-mail: deposit@ccdc.cam.ac.uk or <http://www.ccdc.cam.ac.uk>).

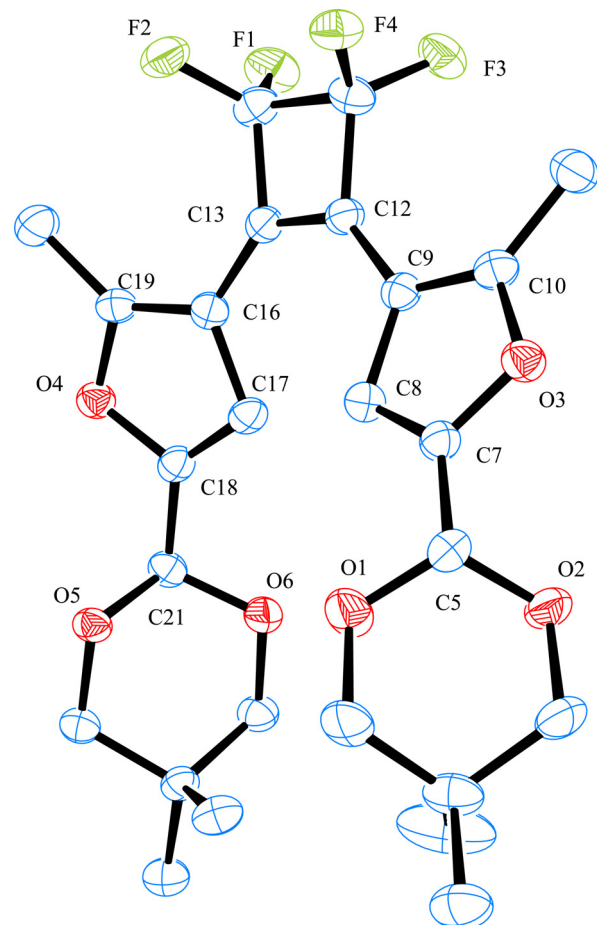


Figure S9. Molecular structure of difurylperfluorocyclobutene **1**. Ellipsoids are drawn at the 50% probability level. Hydrogen atoms are omitted for clarity.

4. Crystallographic Data

Table S2. Crystal data and structure refinement for C4F-NPA (**1**) (CCDC 832576).

Moiety formula	2 (C ₂₆ H ₃₀ F ₈ O ₁₂), 1/2 (C ₆ H ₁₄)	
Formula weight	1072.09	
Temperature	100(2) K	
Wavelength	0.71073 Å	
Crystal system	Triclinic	
Space group	P -1	
Unit cell dimensions	a = 10.9425(16) Å	α = 79.851(10)°.
	b = 12.8801(16) Å	β = 89.064(11)°.
	c = 20.430(3) Å	γ = 73.078(6)°.
Volume	2709.8(7) Å ³	
Z	2	
Density (calculated)	1.314 Mg/m ³	
Absorption coefficient	0.109 mm ⁻¹	
F(000)	1130	
Crystal size	0.400 x 0.300 x 0.200 mm ³	
Theta range for data collection	1.80 to 26.90°.	
Index ranges	-13<=h<=13, -15<=k<=16, -25<=l<=25	
Reflections collected	39119	
Independent reflections	11518 [R(int) = 0.1199]	
Completeness to theta = 26.90°	98.4 %	
Absorption correction	Integration	
Max. and min. transmission	0.9607 and 0.7936	
Refinement method	Full-matrix least-squares on F ²	
Data / restraints / parameters	11518 / 0 / 688	
Goodness-of-fit on F ²	0.938	
Final R indices [I>2sigma(I)]	R1 = 0.0639, wR2 = 0.1060	
R indices (all data)	R1 = 0.1404, wR2 = 0.1269	
Largest diff. peak and hole	0.241 and -0.251 e.Å ⁻³	

4. Crystallographic Data

Table S3. Atomic coordinates ($\times 10^4$) and equivalent isotropic displacement parameters ($\text{\AA}^2 \times 10^3$) for C4F-NPA (1). U(eq) is defined as one third of the trace of the orthogonalized U^{ij} tensor.

	x	y	z	U(eq)
C(1)	8031(3)	-2901(3)	5401(2)	40(1)
C(2)	6872(5)	-2046(4)	4292(2)	72(2)
C(3)	7603(3)	-1848(3)	4865(2)	34(1)
C(4)	6781(3)	-921(3)	5177(2)	36(1)
C(5)	7694(3)	337(2)	4541(2)	26(1)
C(6)	8791(3)	-1521(3)	4616(2)	44(1)
C(7)	7360(3)	1443(2)	4103(1)	25(1)
C(8)	6251(3)	2166(2)	3853(1)	26(1)
C(9)	6560(3)	3123(2)	3489(1)	23(1)
C(10)	7849(3)	2894(2)	3554(1)	26(1)
C(11)	8775(3)	3517(3)	3320(2)	35(1)
C(12)	5677(3)	4164(2)	3180(1)	24(1)
C(13)	4417(3)	4529(2)	3002(1)	23(1)
C(14)	4403(3)	5708(3)	2851(2)	29(1)
C(15)	5848(3)	5292(3)	3009(2)	29(1)
C(16)	3417(3)	4009(2)	2936(1)	24(1)
C(17)	3611(3)	2889(2)	2844(1)	24(1)
C(18)	2448(3)	2766(2)	2792(1)	24(1)
C(19)	2131(3)	4486(2)	2930(1)	25(1)
C(20)	1284(3)	5585(3)	2999(2)	35(1)
C(21)	1970(3)	1822(2)	2700(1)	24(1)
C(22)	1000(3)	525(2)	3247(2)	27(1)
C(23)	2006(3)	-403(2)	3010(1)	24(1)
C(24)	2555(3)	101(2)	2379(2)	28(1)
C(25)	3079(3)	-959(3)	3540(2)	34(1)
C(26)	1369(3)	-1236(3)	2833(2)	33(1)
C(31)	2940(3)	-2932(3)	151(2)	34(1)
C(32)	1619(3)	-2025(3)	1029(2)	36(1)
C(33)	2507(3)	-1893(2)	454(1)	26(1)
C(34)	1811(3)	-921(2)	-82(2)	27(1)
C(35)	2700(3)	272(2)	348(1)	26(1)
C(36)	3690(3)	-1624(3)	688(2)	33(1)
C(37)	2335(3)	1350(2)	573(1)	24(1)
C(38)	1215(3)	2025(2)	704(1)	24(1)
C(39)	1477(3)	2962(2)	903(1)	22(1)
C(40)	2769(3)	2775(2)	862(1)	25(1)
C(41)	3677(3)	3398(3)	982(2)	35(1)
C(42)	556(3)	3929(2)	1051(1)	25(1)
C(43)	-704(3)	4215(2)	1205(1)	25(1)
C(44)	-793(3)	5399(3)	1175(2)	34(1)
C(45)	619(3)	5088(2)	1014(2)	31(1)
C(46)	-1634(3)	3617(2)	1380(1)	24(1)
C(47)	-2933(3)	4044(3)	1337(2)	32(1)
C(48)	-1387(3)	2460(2)	1660(1)	25(1)
C(49)	-2521(3)	2277(3)	1764(2)	28(1)
C(50)	-3852(3)	5127(3)	1051(2)	44(1)
C(51)	-2944(3)	1286(3)	2041(1)	28(1)
C(52)	-2254(3)	-534(3)	2569(2)	42(1)
C(53)	-2980(3)	-881(3)	2062(2)	31(1)
C(54)	-4059(3)	116(3)	1775(2)	34(1)
C(55)	-2089(4)	-1309(3)	1525(2)	54(1)
C(56)	-3538(3)	-1799(3)	2412(2)	40(1)
C(101)	7976(4)	3696(3)	5269(2)	53(1)
C(102)	6834(3)	4718(3)	5178(2)	43(1)
C(103)	5571(3)	4494(3)	5047(2)	38(1)
O(1)	6542(2)	128(2)	4726(1)	37(1)
O(2)	8449(2)	-447(2)	4196(1)	37(1)

4. Crystallographic Data

O(3)	8359(2)	1864(2)	3927(1)	27(1)
O(4)	1520(2)	3722(2)	2843(1)	26(1)
O(5)	1504(2)	1423(2)	3316(1)	25(1)
O(6)	2981(2)	1023(2)	2491(1)	29(1)
O(7)	1566(2)	104(2)	151(1)	27(1)
O(8)	3347(2)	-557(2)	881(1)	30(1)
O(9)	3311(2)	1788(2)	666(1)	28(1)
O(10)	-3492(2)	3230(2)	1574(1)	32(1)
O(11)	-1873(2)	425(2)	2283(1)	39(1)
O(12)	-3610(2)	1056(2)	1528(1)	30(1)
F(1)	4033(2)	6281(2)	2222(1)	39(1)
F(2)	3738(2)	6379(1)	3260(1)	37(1)
F(3)	6582(2)	5478(2)	2480(1)	37(1)
F(4)	6275(2)	5696(1)	3502(1)	35(1)
F(5)	-1576(2)	6152(2)	691(1)	45(1)
F(6)	-1087(2)	5808(2)	1749(1)	41(1)
F(7)	910(2)	5597(2)	411(1)	39(1)
F(8)	1411(2)	5261(2)	1470(1)	37(1)

4. Crystallographic Data

Table S4. Bond lengths [Å] and angles [°] for C4F-NPA (**1**).

C(1)-C(3)	1.544(4)	C(44)-F(6)	1.365(4)
C(2)-C(3)	1.526(5)	C(44)-C(45)	1.524(5)
C(3)-C(4)	1.506(5)	C(45)-F(7)	1.369(3)
C(3)-C(6)	1.532(4)	C(45)-F(8)	1.370(3)
C(4)-O(1)	1.451(3)	C(46)-C(47)	1.365(4)
C(5)-O(2)	1.394(4)	C(46)-C(48)	1.447(4)
C(5)-O(1)	1.397(3)	C(47)-O(10)	1.376(4)
C(5)-C(7)	1.490(4)	C(47)-C(50)	1.488(4)
C(6)-O(2)	1.442(4)	C(48)-C(49)	1.336(4)
C(7)-C(8)	1.340(4)	C(49)-O(10)	1.368(4)
C(7)-O(3)	1.372(3)	C(49)-C(51)	1.498(4)
C(8)-C(9)	1.448(4)	C(51)-O(11)	1.385(4)
C(9)-C(10)	1.358(4)	C(51)-O(12)	1.406(3)
C(9)-C(12)	1.449(4)	C(52)-O(11)	1.442(4)
C(10)-O(3)	1.370(3)	C(52)-C(53)	1.517(5)
C(10)-C(11)	1.490(4)	C(53)-C(54)	1.504(4)
C(12)-C(13)	1.354(4)	C(53)-C(55)	1.523(5)
C(12)-C(15)	1.497(4)	C(53)-C(56)	1.546(4)
C(13)-C(16)	1.458(4)	C(54)-O(12)	1.443(3)
C(13)-C(14)	1.491(4)	C(101)-C(102)	1.515(5)
C(14)-F(2)	1.359(4)	C(102)-C(103)	1.527(5)
C(14)-F(1)	1.366(3)	C(103)-C(103) ^{#1}	1.507(7)
C(14)-C(15)	1.534(4)	C(4)-C(3)-C(2)	110.6(3)
C(15)-F(4)	1.359(3)	C(4)-C(3)-C(6)	107.3(3)
C(15)-F(3)	1.365(3)	C(2)-C(3)-C(6)	110.8(3)
C(16)-C(19)	1.361(4)	C(4)-C(3)-C(1)	109.0(3)
C(16)-C(17)	1.442(4)	C(2)-C(3)-C(1)	110.5(3)
C(17)-C(18)	1.336(4)	C(6)-C(3)-C(1)	108.5(3)
C(18)-O(4)	1.369(3)	O(1)-C(4)-C(3)	111.0(3)
C(18)-C(21)	1.496(4)	O(2)-C(5)-O(1)	112.4(2)
C(19)-O(4)	1.377(3)	O(2)-C(5)-C(7)	109.3(2)
C(19)-C(20)	1.478(4)	O(1)-C(5)-C(7)	106.8(2)
C(21)-O(6)	1.394(3)	O(2)-C(6)-C(3)	111.4(3)
C(21)-O(5)	1.418(3)	C(8)-C(7)-O(3)	110.5(2)
C(22)-O(5)	1.447(3)	C(8)-C(7)-C(5)	133.3(3)
C(22)-C(23)	1.515(4)	O(3)-C(7)-C(5)	116.1(2)
C(23)-C(25)	1.530(4)	C(7)-C(8)-C(9)	106.5(2)
C(23)-C(26)	1.532(4)	C(10)-C(9)-C(8)	106.1(3)
C(23)-C(24)	1.534(4)	C(10)-C(9)-C(12)	126.2(3)
C(24)-O(6)	1.448(3)	C(8)-C(9)-C(12)	127.5(3)
C(31)-C(33)	1.522(4)	C(9)-C(10)-O(3)	110.0(2)
C(32)-C(33)	1.530(4)	C(9)-C(10)-C(11)	134.0(3)
C(33)-C(34)	1.528(4)	O(3)-C(10)-C(11)	116.0(3)
C(33)-C(36)	1.537(4)	C(13)-C(12)-C(9)	135.7(3)
C(34)-O(7)	1.431(4)	C(13)-C(12)-C(15)	93.4(2)
C(35)-O(7)	1.398(3)	C(9)-C(12)-C(15)	130.6(3)
C(35)-O(8)	1.415(3)	C(12)-C(13)-C(16)	135.3(3)
C(35)-C(37)	1.482(4)	C(12)-C(13)-C(14)	93.4(2)
C(36)-O(8)	1.439(4)	C(16)-C(13)-C(14)	131.2(3)
C(37)-C(38)	1.334(4)	F(2)-C(14)-F(1)	104.9(2)
C(37)-O(9)	1.375(3)	F(2)-C(14)-C(13)	117.0(2)
C(38)-C(39)	1.443(4)	F(1)-C(14)-C(13)	118.1(3)
C(39)-C(40)	1.367(4)	F(2)-C(14)-C(15)	113.9(3)
C(39)-C(42)	1.432(4)	F(1)-C(14)-C(15)	116.1(2)
C(40)-O(9)	1.364(4)	C(13)-C(14)-C(15)	86.7(2)
C(40)-C(41)	1.493(4)	F(4)-C(15)-F(3)	105.2(2)
C(42)-C(43)	1.367(4)	F(4)-C(15)-C(12)	117.6(2)
C(42)-C(45)	1.503(4)	F(3)-C(15)-C(12)	117.1(3)
C(43)-C(46)	1.449(4)	F(4)-C(15)-C(14)	116.1(3)
C(43)-C(44)	1.490(4)	F(3)-C(15)-C(14)	114.5(2)
C(44)-F(5)	1.362(3)	C(12)-C(15)-C(14)	86.3(2)

4. Crystallographic Data

C(19)-C(16)-C(17)	106.8(3)	F(5)-C(44)-F(6)	105.5(3)
C(19)-C(16)-C(13)	127.2(3)	F(5)-C(44)-C(43)	117.7(3)
C(17)-C(16)-C(13)	126.1(3)	F(6)-C(44)-C(43)	116.6(2)
C(18)-C(17)-C(16)	106.3(3)	F(5)-C(44)-C(45)	114.5(3)
C(17)-C(18)-O(4)	110.8(3)	F(6)-C(44)-C(45)	115.6(3)
C(17)-C(18)-C(21)	133.9(3)	C(43)-C(44)-C(45)	86.8(2)
O(4)-C(18)-C(21)	115.3(2)	F(7)-C(45)-F(8)	105.2(2)
C(16)-C(19)-O(4)	109.0(3)	F(7)-C(45)-C(42)	116.2(3)
C(16)-C(19)-C(20)	135.5(3)	F(8)-C(45)-C(42)	117.3(2)
O(4)-C(19)-C(20)	115.5(3)	F(7)-C(45)-C(44)	115.8(2)
O(6)-C(21)-O(5)	112.3(2)	F(8)-C(45)-C(44)	115.1(3)
O(6)-C(21)-C(18)	108.0(2)	C(42)-C(45)-C(44)	87.2(2)
O(5)-C(21)-C(18)	107.9(2)	C(47)-C(46)-C(48)	105.5(3)
O(5)-C(22)-C(23)	111.3(2)	C(47)-C(46)-C(43)	126.9(3)
C(22)-C(23)-C(25)	111.0(3)	C(48)-C(46)-C(43)	127.5(3)
C(22)-C(23)-C(26)	109.0(2)	C(46)-C(47)-O(10)	109.9(3)
C(25)-C(23)-C(26)	111.0(2)	C(46)-C(47)-C(50)	135.4(3)
C(22)-C(23)-C(24)	107.4(2)	O(10)-C(47)-C(50)	114.5(3)
C(25)-C(23)-C(24)	109.5(2)	C(49)-C(48)-C(46)	107.1(3)
C(26)-C(23)-C(24)	108.8(2)	C(48)-C(49)-O(10)	110.6(3)
O(6)-C(24)-C(23)	111.2(2)	C(48)-C(49)-C(51)	134.5(3)
C(31)-C(33)-C(34)	109.3(3)	O(10)-C(49)-C(51)	114.9(2)
C(31)-C(33)-C(32)	111.3(3)	O(11)-C(51)-O(12)	112.8(3)
C(34)-C(33)-C(32)	109.6(3)	O(11)-C(51)-C(49)	108.3(2)
C(31)-C(33)-C(36)	109.0(2)	O(12)-C(51)-C(49)	107.7(2)
C(34)-C(33)-C(36)	106.6(2)	O(11)-C(52)-C(53)	111.3(2)
C(32)-C(33)-C(36)	111.0(3)	C(54)-C(53)-C(52)	107.1(3)
O(7)-C(34)-C(33)	111.3(2)	C(54)-C(53)-C(55)	111.5(3)
O(7)-C(35)-O(8)	111.9(2)	C(52)-C(53)-C(55)	110.1(3)
O(7)-C(35)-C(37)	106.5(2)	C(54)-C(53)-C(56)	109.1(3)
O(8)-C(35)-C(37)	108.8(2)	C(52)-C(53)-C(56)	109.6(2)
O(8)-C(36)-C(33)	111.3(2)	C(55)-C(53)-C(56)	109.4(3)
C(38)-C(37)-O(9)	110.5(3)	O(12)-C(54)-C(53)	111.7(2)
C(38)-C(37)-C(35)	133.0(3)	C(101)-C(102)-C(103)	113.7(3)
O(9)-C(37)-C(35)	116.5(2)	C(103)#1-C(103)-C(102)	114.1(4)
C(37)-C(38)-C(39)	107.0(2)	C(5)-O(1)-C(4)	110.4(2)
C(40)-C(39)-C(42)	127.4(3)	C(5)-O(2)-C(6)	109.9(2)
C(40)-C(39)-C(38)	105.6(3)	C(7)-O(3)-C(10)	107.0(2)
C(42)-C(39)-C(38)	126.7(3)	C(18)-O(4)-C(19)	107.1(2)
O(9)-C(40)-C(39)	110.0(2)	C(21)-O(5)-C(22)	109.9(2)
O(9)-C(40)-C(41)	115.3(3)	C(21)-O(6)-C(24)	110.0(2)
C(39)-C(40)-C(41)	134.6(3)	C(35)-O(7)-C(34)	111.2(2)
C(43)-C(42)-C(39)	136.1(3)	C(35)-O(8)-C(36)	110.6(2)
C(43)-C(42)-C(45)	92.3(3)	C(40)-O(9)-C(37)	106.9(2)
C(39)-C(42)-C(45)	131.3(3)	C(49)-O(10)-C(47)	106.9(2)
C(42)-C(43)-C(46)	135.0(3)	C(51)-O(11)-C(52)	109.6(2)
C(42)-C(43)-C(44)	93.8(2)	C(51)-O(12)-C(54)	109.8(2)
C(46)-C(43)-C(44)	131.2(3)		

Symmetry transformations used to generate equivalent atoms:

#1 -x+1,-y+1,-z+1

4. Crystallographic Data

Table S5. Anisotropic displacement parameters ($\text{\AA}^2 \times 10^3$) for C4F-NPA (**1**). The anisotropic displacement factor exponent takes the form: $-2\pi^2 [h^2 a^* U^{11} + \dots + 2 h k a^* b^* U^{12}]$

	U ¹¹	U ²²	U ³³	U ²³	U ¹³	U ¹²
C(1)	59(2)	30(2)	31(2)	1(2)	2(2)	-14(2)
C(2)	132(4)	61(3)	36(2)	12(2)	-29(2)	-60(3)
C(3)	53(2)	30(2)	22(2)	1(1)	-4(1)	-19(2)
C(4)	38(2)	30(2)	33(2)	13(2)	0(1)	-8(2)
C(5)	26(2)	24(2)	27(2)	-6(1)	-1(1)	-4(1)
C(6)	51(2)	19(2)	52(2)	0(2)	16(2)	-1(2)
C(7)	26(2)	22(2)	25(2)	-3(1)	2(1)	-6(1)
C(8)	26(2)	25(2)	26(2)	-5(1)	1(1)	-8(1)
C(9)	27(2)	23(2)	21(2)	-7(1)	2(1)	-8(1)
C(10)	31(2)	22(2)	25(2)	-3(1)	-1(1)	-7(1)
C(11)	30(2)	30(2)	46(2)	-1(2)	1(2)	-12(2)
C(12)	27(2)	20(2)	24(2)	-4(1)	2(1)	-6(1)
C(13)	27(2)	21(2)	19(2)	-2(1)	3(1)	-5(1)
C(14)	37(2)	23(2)	24(2)	-1(1)	-1(1)	-6(1)
C(15)	35(2)	29(2)	25(2)	-4(1)	-1(1)	-15(2)
C(16)	27(2)	21(2)	19(2)	3(1)	1(1)	-5(1)
C(17)	29(2)	19(2)	21(2)	1(1)	0(1)	-3(1)
C(18)	28(2)	21(2)	22(2)	-2(1)	1(1)	-4(1)
C(19)	30(2)	21(2)	25(2)	-1(1)	-1(1)	-8(1)
C(20)	30(2)	26(2)	46(2)	-5(2)	0(2)	-4(1)
C(21)	27(2)	25(2)	21(2)	1(1)	-1(1)	-8(1)
C(22)	30(2)	24(2)	25(2)	0(1)	1(1)	-9(1)
C(23)	26(2)	20(2)	24(2)	-1(1)	-1(1)	-4(1)
C(24)	35(2)	26(2)	28(2)	-8(1)	2(1)	-13(1)
C(25)	42(2)	24(2)	34(2)	-2(1)	-5(2)	-7(2)
C(26)	40(2)	29(2)	33(2)	-5(1)	-1(1)	-13(2)
C(31)	38(2)	28(2)	38(2)	-8(2)	-1(2)	-9(2)
C(32)	50(2)	36(2)	26(2)	-5(1)	7(2)	-18(2)
C(33)	29(2)	24(2)	24(2)	-2(1)	0(1)	-9(1)
C(34)	32(2)	24(2)	26(2)	-4(1)	-1(1)	-10(1)
C(35)	25(2)	30(2)	24(2)	0(1)	-1(1)	-10(1)
C(36)	37(2)	26(2)	34(2)	-5(1)	-6(1)	-4(2)
C(37)	28(2)	28(2)	19(2)	2(1)	0(1)	-14(1)
C(38)	27(2)	24(2)	21(2)	2(1)	-2(1)	-14(1)
C(39)	28(2)	23(2)	18(1)	1(1)	0(1)	-13(1)
C(40)	32(2)	25(2)	21(2)	-1(1)	1(1)	-13(1)
C(41)	35(2)	39(2)	36(2)	-7(2)	-1(1)	-20(2)
C(42)	32(2)	26(2)	16(1)	3(1)	-5(1)	-13(1)
C(43)	35(2)	21(2)	18(1)	-2(1)	-5(1)	-7(1)
C(44)	49(2)	26(2)	26(2)	0(1)	-3(2)	-11(2)
C(45)	49(2)	24(2)	22(2)	2(1)	-4(1)	-18(2)
C(46)	30(2)	24(2)	20(2)	-7(1)	-3(1)	-8(1)
C(47)	31(2)	31(2)	34(2)	-12(1)	-6(1)	-7(2)
C(48)	26(2)	24(2)	25(2)	-6(1)	-3(1)	-7(1)
C(49)	28(2)	31(2)	25(2)	-9(1)	0(1)	-7(1)
C(50)	32(2)	34(2)	59(2)	-8(2)	-9(2)	-1(2)
C(51)	29(2)	39(2)	20(2)	-7(1)	4(1)	-14(2)
C(52)	44(2)	49(2)	37(2)	14(2)	-7(2)	-30(2)
C(53)	38(2)	31(2)	25(2)	2(1)	3(1)	-15(2)
C(54)	35(2)	31(2)	41(2)	-7(2)	-3(2)	-17(2)
C(55)	72(3)	29(2)	49(2)	3(2)	20(2)	-5(2)
C(56)	50(2)	42(2)	33(2)	3(2)	-3(2)	-26(2)
C(101)	53(2)	57(3)	44(2)	-10(2)	1(2)	-9(2)
C(102)	54(2)	44(2)	32(2)	-3(2)	1(2)	-16(2)
C(103)	54(2)	35(2)	26(2)	-6(2)	4(2)	-14(2)
O(1)	30(1)	32(1)	39(1)	12(1)	2(1)	-6(1)
O(2)	47(1)	20(1)	37(1)	-2(1)	16(1)	-4(1)

4. Crystallographic Data

O(3)	26(1)	26(1)	28(1)	0(1)	0(1)	-8(1)
O(4)	26(1)	23(1)	27(1)	-1(1)	0(1)	-7(1)
O(5)	32(1)	23(1)	20(1)	-2(1)	3(1)	-10(1)
O(6)	31(1)	26(1)	32(1)	-9(1)	6(1)	-12(1)
O(7)	31(1)	23(1)	27(1)	-5(1)	-5(1)	-8(1)
O(8)	34(1)	24(1)	29(1)	-5(1)	-7(1)	-6(1)
O(9)	26(1)	33(1)	29(1)	-6(1)	2(1)	-13(1)
O(10)	26(1)	34(1)	38(1)	-11(1)	0(1)	-9(1)
O(11)	35(1)	42(1)	39(1)	14(1)	-9(1)	-23(1)
O(12)	33(1)	29(1)	30(1)	-5(1)	-7(1)	-12(1)
F(1)	46(1)	33(1)	33(1)	13(1)	-8(1)	-12(1)
F(2)	39(1)	23(1)	48(1)	-9(1)	1(1)	-5(1)
F(3)	39(1)	38(1)	36(1)	2(1)	6(1)	-18(1)
F(4)	40(1)	28(1)	39(1)	-7(1)	-4(1)	-14(1)
F(5)	55(1)	27(1)	43(1)	8(1)	-6(1)	-4(1)
F(6)	57(1)	32(1)	40(1)	-15(1)	9(1)	-18(1)
F(7)	62(1)	31(1)	27(1)	5(1)	4(1)	-22(1)
F(8)	49(1)	37(1)	32(1)	-7(1)	-3(1)	-24(1)

4. Crystallographic Data

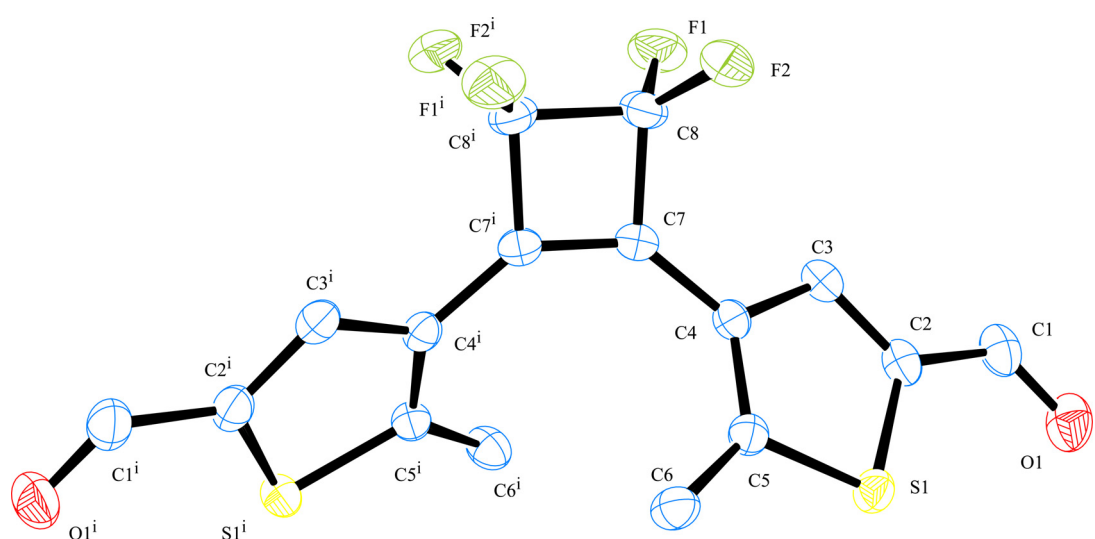


Figure S10. Molecular structure of dithienyl perfluorocyclobutene **5**. Ellipsoids are drawn at the 50% probability level. Hydrogen atoms are omitted for clarity.

4. Crystallographic Data

Table S6. Crystal data and structure refinement for C4F-T-CHO (**5**) (CCDC 832577).

Empirical formula	C16 H10 F4 O2 S2		
Formula weight	374.36		
Temperature	100(2) K		
Wavelength	0.71073 Å		
Crystal system	Monoclinic		
Space group	C 2/c		
Unit cell dimensions	$a = 21.146(3)$ Å	$\alpha = 90^\circ$.	
	$b = 8.0742(8)$ Å	$\beta = 112.593(12)^\circ$.	
	$c = 9.9346(17)$ Å	$\gamma = 90^\circ$.	
Volume	1566.0(4) Å ³		
Z	4		
Density (calculated)	1.588 Mg/m ³		
Absorption coefficient	0.390 mm ⁻¹		
F(000)	760		
Crystal size	0.400 x 0.300 x 0.200 mm ³		
Theta range for data collection	2.09 to 26.71°.		
Index ranges	-26<=h<=26, -10<=k<=10, -12<=l<=12		
Reflections collected	9953		
Independent reflections	1648 [R(int) = 0.0813]		
Completeness to theta = 26.71°	99.5 %		
Absorption correction	Integration		
Max. and min. transmission	0.9834 and 0.9073		
Refinement method	Full-matrix least-squares on F ²		
Data / restraints / parameters	1648 / 0 / 110		
Goodness-of-fit on F ²	1.078		
Final R indices [I>2sigma(I)]	R1 = 0.0380, wR2 = 0.0902		
R indices (all data)	R1 = 0.0500, wR2 = 0.0939		
Largest diff. peak and hole	0.312 and -0.269 e.Å ⁻³		

4. Crystallographic Data

Table S7. Atomic coordinates ($\times 10^4$) and equivalent isotropic displacement parameters ($\text{\AA}^2 \times 10^3$) for C4F-T-CHO (5). U(eq) is defined as one third of the trace of the orthogonalized U^{ij} tensor.

	x	y	z	U(eq)
F(1)	394(1)	3656(2)	4394(1)	41(1)
F(2)	856(1)	3536(2)	2791(2)	40(1)
O(1)	2916(1)	9268(2)	7318(2)	40(1)
S(1)	1725(1)	9761(1)	4354(1)	26(1)
C(1)	2484(1)	8192(3)	6974(2)	32(1)
C(2)	1880(1)	8180(3)	5613(2)	26(1)
C(3)	1396(1)	6971(3)	5140(2)	25(1)
C(4)	877(1)	7331(2)	3741(2)	21(1)
C(5)	996(1)	8807(2)	3175(2)	23(1)
C(6)	611(1)	9524(3)	1695(2)	29(1)
C(7)	328(1)	6168(2)	2994(2)	22(1)
C(8)	361(1)	4310(2)	3108(2)	28(1)

4. Crystallographic Data

Table S8. Bond lengths [Å] and angles [°] for C4F-T-CHO (**5**).

F(1)-C(8)	1.360(2)
F(2)-C(8)	1.356(2)
O(1)-C(1)	1.211(3)
S(1)-C(5)	1.7188(19)
S(1)-C(2)	1.729(2)
C(1)-C(2)	1.460(3)
C(2)-C(3)	1.362(3)
C(3)-C(4)	1.431(3)
C(4)-C(5)	1.381(3)
C(4)-C(7)	1.456(3)
C(5)-C(6)	1.497(3)
C(7)-C(7)#1	1.357(4)
C(7)-C(8)	1.503(3)
C(8)-C(8)#1	1.540(4)
C(5)-S(1)-C(2)	91.90(10)
O(1)-C(1)-C(2)	124.3(2)
C(3)-C(2)-C(1)	126.8(2)
C(3)-C(2)-S(1)	111.80(15)
C(1)-C(2)-S(1)	121.35(17)
C(2)-C(3)-C(4)	112.55(18)
C(5)-C(4)-C(3)	112.32(17)
C(5)-C(4)-C(7)	125.70(17)
C(3)-C(4)-C(7)	121.80(18)
C(4)-C(5)-C(6)	128.18(18)
C(4)-C(5)-S(1)	111.41(14)
C(6)-C(5)-S(1)	120.21(15)
C(7)#1-C(7)-C(4)	139.67(10)
C(7)#1-C(7)-C(8)	93.41(11)
C(4)-C(7)-C(8)	126.89(17)
F(2)-C(8)-F(1)	105.84(16)
F(2)-C(8)-C(7)	117.43(18)
F(1)-C(8)-C(7)	116.26(17)
F(2)-C(8)-C(8)#1	116.1(2)
F(1)-C(8)-C(8)#1	114.5(2)
C(7)-C(8)-C(8)#1	86.42(11)

Symmetry transformations used to generate equivalent atoms:

#1 -x,y,-z+1/2

4. Crystallographic Data

Table S9. Anisotropic displacement parameters ($\text{\AA}^2 \times 10^3$) for C4F-T-CHO (**5**). The anisotropic displacement factor exponent takes the form: $-2\pi^2 [h^2 a^* U^{11} + \dots + 2 h k a^* b^* U^{12}]$

	U ¹¹	U ²²	U ³³	U ²³	U ¹³	U ¹²
F(1)	51(1)	30(1)	39(1)	14(1)	14(1)	1(1)
F(2)	36(1)	26(1)	59(1)	-4(1)	20(1)	7(1)
O(1)	31(1)	47(1)	35(1)	-13(1)	4(1)	-3(1)
S(1)	23(1)	26(1)	28(1)	-4(1)	7(1)	-3(1)
C(1)	26(1)	38(1)	28(1)	-7(1)	6(1)	5(1)
C(2)	23(1)	30(1)	23(1)	-2(1)	7(1)	5(1)
C(3)	25(1)	25(1)	24(1)	2(1)	9(1)	6(1)
C(4)	20(1)	22(1)	22(1)	0(1)	9(1)	3(1)
C(5)	22(1)	23(1)	24(1)	-2(1)	9(1)	0(1)
C(6)	32(1)	26(1)	25(1)	2(1)	8(1)	-5(1)
C(7)	26(1)	19(1)	22(1)	1(1)	10(1)	1(1)
C(8)	31(1)	19(1)	34(1)	3(1)	13(1)	4(1)

4. Crystallographic Data

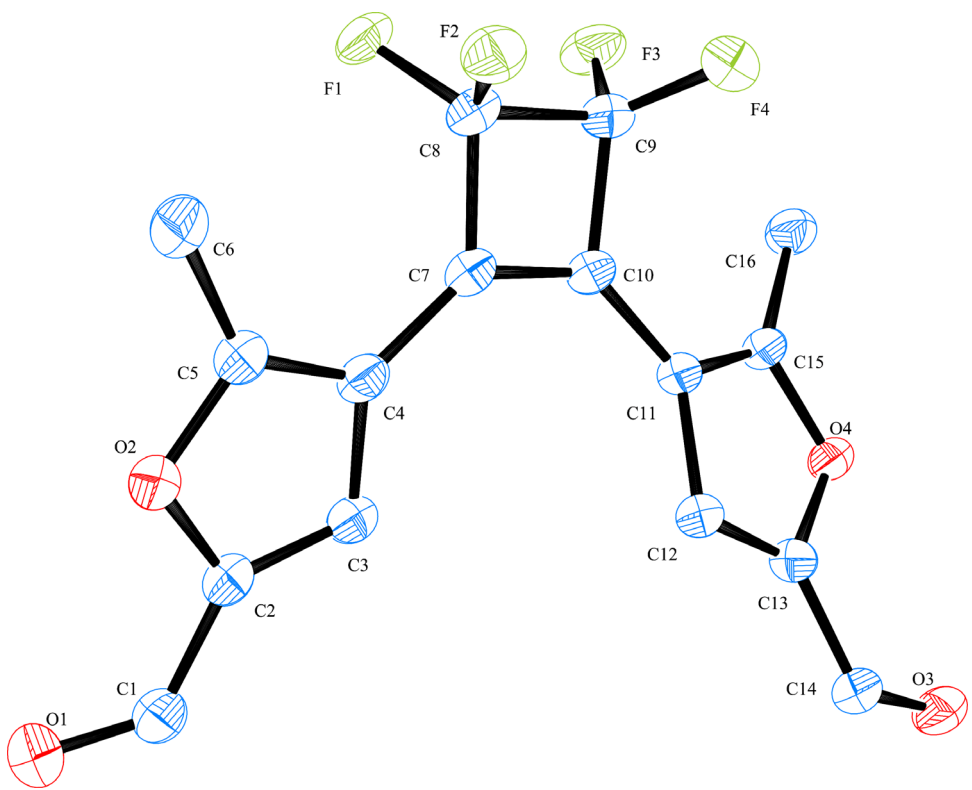


Figure S11. Molecular structure of difurylperfluorocyclobutene **2**. Ellipsoids are drawn at the 50% probability level. Hydrogen atoms are omitted for clarity.

4. Crystallographic Data

Table S10. Crystal data and structure refinement for C4F-CHO (**2**) (CCDC 856183).

Empirical formula	C16 H10 F4 O4
Formula weight	342.24
Temperature	100(2) K
Wavelength	0.71073 Å
Crystal system	Triclinic
Space group	P -1
Unit cell dimensions	$a = 7.7690(8)$ Å $\alpha = 92.603(8)^\circ$. $b = 11.4753(12)$ Å $\beta = 90.925(8)^\circ$. $c = 16.5918(17)$ Å $\gamma = 106.115(8)^\circ$.
Volume	1419.0(3) Å ³
Z	4
Density (calculated)	1.602 Mg/m ³
Absorption coefficient	0.148 mm ⁻¹
F(000)	696
Crystal size	0.450 x 0.377 x 0.300 mm ³
Theta range for data collection	1.85 to 26.80°.
Index ranges	-9<=h<=9, -14<=k<=14, -21<=l<=21
Reflections collected	18618
Independent reflections	5985 [R(int) = 0.0688]
Completeness to theta = 26.80°	98.9 %
Absorption correction	Integration
Max. and min. transmission	0.9692 and 0.9392
Refinement method	Full-matrix least-squares on F ²
Data / restraints / parameters	5985 / 0 / 437
Goodness-of-fit on F ²	1.017
Final R indices [I>2sigma(I)]	R1 = 0.0450, wR2 = 0.1073
R indices (all data)	R1 = 0.0653, wR2 = 0.1152
Largest diff. peak and hole	0.313 and -0.246 e.Å ⁻³

4. Crystallographic Data

Table S11. Atomic coordinates ($\times 10^4$) and equivalent isotropic displacement parameters ($\text{\AA}^2 \times 10^3$) for C4F-CHO (2). U(eq) is defined as one third of the trace of the orthogonalized U^{ij} tensor.

	x	y	z	U(eq)
C(1)	5866(3)	7953(2)	8019(1)	29(1)
C(2)	6227(2)	7356(2)	7283(1)	26(1)
C(3)	6095(2)	7612(2)	6498(1)	25(1)
C(4)	6726(2)	6747(2)	6032(1)	25(1)
C(5)	7188(3)	6005(2)	6572(1)	27(1)
C(6)	7943(3)	4953(2)	6496(1)	34(1)
C(7)	6947(2)	6693(2)	5166(1)	24(1)
C(8)	7942(3)	5985(2)	4661(1)	26(1)
C(9)	7470(3)	6643(2)	3939(1)	27(1)
C(10)	6484(2)	7243(2)	4523(1)	24(1)
C(11)	5360(2)	8037(2)	4372(1)	22(1)
C(12)	3863(2)	8172(2)	4823(1)	24(1)
C(13)	3180(2)	8957(2)	4428(1)	24(1)
C(14)	1625(3)	9394(2)	4582(1)	28(1)
C(15)	5462(2)	8754(2)	3724(1)	23(1)
C(16)	6674(3)	9004(2)	3031(1)	29(1)
C(17)	-3527(3)	9327(2)	522(1)	29(1)
C(18)	-1941(3)	8930(2)	682(1)	26(1)
C(19)	-1221(3)	8151(2)	262(1)	25(1)
C(20)	272(2)	8039(2)	738(1)	23(1)
C(21)	348(2)	8765(2)	1426(1)	25(1)
C(22)	1531(3)	9023(2)	2166(1)	33(1)
C(23)	1421(2)	7251(2)	575(1)	24(1)
C(24)	2418(3)	6684(2)	1150(1)	28(1)
C(25)	2905(3)	6006(2)	408(1)	28(1)
C(26)	1889(2)	6675(2)	-86(1)	25(1)
C(27)	1683(2)	6706(2)	-953(1)	24(1)
C(28)	1059(2)	7557(2)	-1391(1)	26(1)
C(29)	1253(2)	7305(2)	-2186(1)	26(1)
C(30)	981(3)	7928(2)	-2893(1)	30(1)
C(31)	2202(3)	5972(2)	-1523(1)	27(1)
C(32)	2971(3)	4929(2)	-1485(1)	35(1)
O(1)	6209(2)	7706(2)	8695(1)	37(1)
O(2)	6897(2)	6362(1)	7337(1)	28(1)
O(3)	1114(2)	10067(1)	4148(1)	33(1)
O(4)	4153(2)	9332(1)	3753(1)	25(1)
O(5)	-4097(2)	9977(1)	983(1)	36(1)
O(6)	-983(2)	9327(1)	1399(1)	27(1)
O(7)	1430(2)	7726(2)	-3567(1)	39(1)
O(8)	1950(2)	6326(1)	-2274(1)	28(1)
F(1)	9720(2)	6200(1)	4830(1)	32(1)
F(2)	7249(2)	4761(1)	4596(1)	32(1)
F(3)	8920(2)	7358(1)	3579(1)	36(1)
F(4)	6467(2)	5921(1)	3331(1)	35(1)
F(5)	1431(2)	5980(1)	1708(1)	36(1)
F(6)	3870(2)	7420(1)	1568(1)	38(1)
F(7)	2238(2)	4776(1)	406(1)	33(1)
F(8)	4682(2)	6229(1)	277(1)	34(1)

4. Crystallographic Data

Table S12. Bond lengths [\AA] and angles [$^\circ$] for C4F-CHO (**2**).

C(1)-O(1)	1.213(2)	O(2)-C(5)-C(6)	115.63(17)
C(1)-C(2)	1.442(3)	C(4)-C(5)-C(6)	134.20(18)
C(2)-C(3)	1.356(3)	C(10)-C(7)-C(4)	136.56(18)
C(2)-O(2)	1.386(2)	C(10)-C(7)-C(8)	93.35(16)
C(3)-C(4)	1.427(3)	C(4)-C(7)-C(8)	130.02(17)
C(4)-C(5)	1.374(3)	F(2)-C(8)-F(1)	106.47(16)
C(4)-C(7)	1.450(3)	F(2)-C(8)-C(7)	117.14(16)
C(5)-O(2)	1.357(2)	F(1)-C(8)-C(7)	116.95(16)
C(5)-C(6)	1.483(3)	F(2)-C(8)-C(9)	114.03(16)
C(7)-C(10)	1.356(3)	F(1)-C(8)-C(9)	115.23(16)
C(7)-C(8)	1.507(3)	C(7)-C(8)-C(9)	86.44(14)
C(8)-F(2)	1.356(2)	F(4)-C(9)-F(3)	105.43(15)
C(8)-F(1)	1.356(2)	F(4)-C(9)-C(10)	116.47(16)
C(8)-C(9)	1.537(3)	F(3)-C(9)-C(10)	118.06(17)
C(9)-F(4)	1.360(2)	F(4)-C(9)-C(8)	115.93(17)
C(9)-F(3)	1.361(2)	F(3)-C(9)-C(8)	114.05(16)
C(9)-C(10)	1.502(3)	C(10)-C(9)-C(8)	86.66(14)
C(10)-C(11)	1.453(3)	C(7)-C(10)-C(11)	136.75(17)
C(11)-C(15)	1.373(3)	C(7)-C(10)-C(9)	93.50(16)
C(11)-C(12)	1.432(3)	C(11)-C(10)-C(9)	129.58(17)
C(12)-C(13)	1.353(3)	C(15)-C(11)-C(12)	106.22(17)
C(13)-O(4)	1.380(2)	C(15)-C(11)-C(10)	125.84(17)
C(13)-C(14)	1.453(3)	C(12)-C(11)-C(10)	127.81(17)
C(14)-O(3)	1.218(3)	C(13)-C(12)-C(11)	106.45(17)
C(15)-O(4)	1.360(2)	C(12)-C(13)-O(4)	110.40(16)
C(15)-C(16)	1.485(3)	C(12)-C(13)-C(14)	131.27(18)
C(17)-O(5)	1.216(3)	O(4)-C(13)-C(14)	118.28(17)
C(17)-C(18)	1.452(3)	O(3)-C(14)-C(13)	124.12(19)
C(18)-C(19)	1.353(3)	O(4)-C(15)-C(11)	110.13(16)
C(18)-O(6)	1.383(2)	O(4)-C(15)-C(16)	116.48(17)
C(19)-C(20)	1.431(3)	C(11)-C(15)-C(16)	133.39(18)
C(20)-C(21)	1.372(3)	O(5)-C(17)-C(18)	124.51(19)
C(20)-C(23)	1.456(3)	C(19)-C(18)-O(6)	110.18(17)
C(21)-O(6)	1.363(2)	C(19)-C(18)-C(17)	131.29(18)
C(21)-C(22)	1.490(3)	O(6)-C(18)-C(17)	118.42(17)
C(23)-C(26)	1.362(3)	C(18)-C(19)-C(20)	106.66(17)
C(23)-C(24)	1.500(3)	C(21)-C(20)-C(19)	106.28(17)
C(24)-F(5)	1.358(2)	C(21)-C(20)-C(23)	125.52(17)
C(24)-F(6)	1.364(2)	C(19)-C(20)-C(23)	128.05(17)
C(24)-C(25)	1.536(3)	O(6)-C(21)-C(20)	110.09(16)
C(25)-F(8)	1.355(2)	O(6)-C(21)-C(22)	116.51(17)
C(25)-F(7)	1.362(2)	C(20)-C(21)-C(22)	133.39(18)
C(25)-C(26)	1.502(3)	C(26)-C(23)-C(20)	136.57(18)
C(26)-C(27)	1.447(3)	C(26)-C(23)-C(24)	93.43(16)
C(27)-C(31)	1.377(3)	C(20)-C(23)-C(24)	129.79(17)
C(27)-C(28)	1.426(3)	F(5)-C(24)-F(6)	105.36(15)
C(28)-C(29)	1.356(3)	F(5)-C(24)-C(23)	116.68(16)
C(29)-O(8)	1.379(2)	F(6)-C(24)-C(23)	118.19(17)
C(29)-C(30)	1.444(3)	F(5)-C(24)-C(25)	116.05(17)
C(30)-O(7)	1.209(3)	F(6)-C(24)-C(25)	113.66(16)
C(31)-O(8)	1.356(2)	C(23)-C(24)-C(25)	86.66(15)
C(31)-C(32)	1.482(3)	F(8)-C(25)-F(7)	106.14(16)
O(1)-C(1)-C(2)	125.3(2)	F(8)-C(25)-C(26)	116.92(17)
C(3)-C(2)-O(2)	109.85(17)	F(7)-C(25)-C(26)	117.06(16)
C(3)-C(2)-C(1)	131.59(19)	F(8)-C(25)-C(24)	115.55(16)
O(2)-C(2)-C(1)	118.51(17)	F(7)-C(25)-C(24)	114.04(16)
C(2)-C(3)-C(4)	106.80(18)	C(26)-C(25)-C(24)	86.68(15)
C(5)-C(4)-C(3)	106.28(17)	C(23)-C(26)-C(27)	136.35(19)
C(5)-C(4)-C(7)	126.13(18)	C(23)-C(26)-C(25)	93.20(16)
C(3)-C(4)-C(7)	127.50(18)	C(27)-C(26)-C(25)	130.29(18)
O(2)-C(5)-C(4)	110.15(17)	C(31)-C(27)-C(28)	105.95(17)

4. Crystallographic Data

C(31)-C(27)-C(26)	126.23(19)	O(8)-C(31)-C(27)	110.09(18)
C(28)-C(27)-C(26)	127.61(18)	O(8)-C(31)-C(32)	115.74(17)
C(29)-C(28)-C(27)	106.97(18)	C(27)-C(31)-C(32)	134.16(19)
C(28)-C(29)-O(8)	109.79(17)	C(5)-O(2)-C(2)	106.93(15)
C(28)-C(29)-C(30)	131.1(2)	C(15)-O(4)-C(13)	106.79(15)
O(8)-C(29)-C(30)	118.93(17)	C(21)-O(6)-C(18)	106.77(15)
O(7)-C(30)-C(29)	125.7(2)	C(31)-O(8)-C(29)	107.19(15)

4. Crystallographic Data

Table S13. Anisotropic displacement parameters ($\text{\AA}^2 \times 10^3$) for C4F-CHO (**2**). The anisotropic displacement factor exponent takes the form: $-2\pi^2 [h^2 a^* U^{11} + \dots + 2 h k a^* b^* U^{12}]$

	U ¹¹	U ²²	U ³³	U ²³	U ¹³	U ¹²
C(1)	21(1)	33(1)	30(1)	0(1)	0(1)	7(1)
C(2)	20(1)	30(1)	29(1)	2(1)	-1(1)	8(1)
C(3)	21(1)	29(1)	27(1)	2(1)	2(1)	10(1)
C(4)	19(1)	28(1)	28(1)	3(1)	2(1)	9(1)
C(5)	22(1)	31(1)	28(1)	1(1)	0(1)	9(1)
C(6)	38(1)	37(1)	33(1)	2(1)	-4(1)	20(1)
C(7)	19(1)	26(1)	28(1)	2(1)	2(1)	8(1)
C(8)	22(1)	28(1)	31(1)	1(1)	2(1)	12(1)
C(9)	25(1)	31(1)	26(1)	0(1)	4(1)	12(1)
C(10)	18(1)	29(1)	25(1)	0(1)	2(1)	8(1)
C(11)	19(1)	26(1)	22(1)	-2(1)	1(1)	8(1)
C(12)	20(1)	29(1)	23(1)	0(1)	2(1)	9(1)
C(13)	22(1)	28(1)	23(1)	-1(1)	2(1)	8(1)
C(14)	24(1)	33(1)	29(1)	-1(1)	1(1)	12(1)
C(15)	19(1)	27(1)	26(1)	-2(1)	0(1)	10(1)
C(16)	26(1)	38(1)	27(1)	6(1)	5(1)	13(1)
C(17)	26(1)	31(1)	32(1)	1(1)	-2(1)	12(1)
C(18)	26(1)	29(1)	24(1)	-1(1)	0(1)	10(1)
C(19)	23(1)	29(1)	26(1)	1(1)	0(1)	10(1)
C(20)	20(1)	27(1)	25(1)	2(1)	1(1)	8(1)
C(21)	21(1)	28(1)	28(1)	1(1)	1(1)	10(1)
C(22)	30(1)	40(1)	30(1)	-6(1)	-5(1)	13(1)
C(23)	20(1)	28(1)	27(1)	-1(1)	-1(1)	8(1)
C(24)	24(1)	32(1)	28(1)	0(1)	-3(1)	9(1)
C(25)	20(1)	29(1)	35(1)	1(1)	-1(1)	9(1)
C(26)	18(1)	26(1)	30(1)	0(1)	1(1)	7(1)
C(27)	17(1)	28(1)	29(1)	0(1)	1(1)	8(1)
C(28)	20(1)	28(1)	30(1)	0(1)	2(1)	7(1)
C(29)	19(1)	28(1)	33(1)	1(1)	2(1)	6(1)
C(30)	24(1)	33(1)	34(1)	5(1)	5(1)	8(1)
C(31)	22(1)	30(1)	29(1)	1(1)	1(1)	7(1)
C(32)	40(1)	38(1)	33(1)	1(1)	6(1)	21(1)
O(1)	39(1)	47(1)	27(1)	-1(1)	-3(1)	16(1)
O(2)	27(1)	34(1)	25(1)	3(1)	0(1)	12(1)
O(3)	30(1)	39(1)	36(1)	2(1)	2(1)	19(1)
O(4)	21(1)	31(1)	24(1)	3(1)	1(1)	12(1)
O(5)	34(1)	39(1)	40(1)	-6(1)	0(1)	21(1)
O(6)	25(1)	31(1)	27(1)	-3(1)	-1(1)	12(1)
O(7)	39(1)	49(1)	31(1)	7(1)	8(1)	17(1)
O(8)	26(1)	32(1)	27(1)	1(1)	3(1)	12(1)
F(1)	21(1)	39(1)	39(1)	2(1)	1(1)	16(1)
F(2)	35(1)	27(1)	37(1)	1(1)	2(1)	13(1)
F(3)	29(1)	43(1)	40(1)	11(1)	14(1)	16(1)
F(4)	38(1)	41(1)	29(1)	-5(1)	-1(1)	16(1)
F(5)	40(1)	43(1)	31(1)	8(1)	4(1)	17(1)
F(6)	30(1)	43(1)	41(1)	-9(1)	-13(1)	14(1)
F(7)	34(1)	28(1)	38(1)	1(1)	0(1)	13(1)
F(8)	20(1)	41(1)	43(1)	2(1)	-1(1)	15(1)

5. Quantum Mechanical Calculation

We performed theoretical calculations of the different conformations in the ground and excited states using Density Functional Theory (DFT) as well as Complete Active Space Multiconfiguration SCF (CASSCF) with the Gaussian 09 program package.^[11]

DFT Calculations:

The reactive and non-reactive open as well as the closed form were optimized at the B3LYP^[12]/6-31g(d,p)^[13] level of theory. Additionally, the transformation from the non-reactive to the reactive conformation and from the open to the closed form was simulated by relaxed potential energy scans followed by energy optimizations to the transition states in the electronic ground state. Both torsion angles (C4-C7 and C4ⁱ-C7ⁱ) were changed simultaneously to get from the reactive to the non-reactive state. Therefore, the given barrier is an upper bound since a stepwise transformation is more likely. This estimate is already sufficient for the qualitative given below. For an accurate description of the chemical reaction, unrestricted DFT (uB3LYP/6-31g(d,p) with the additional keywords “Guess=(Mix,Always)”) was needed to be able to describe the homolytic breaking of the bond. Convergence to a local minimum or transition state was verified by the absence or presence of one imaginary frequency in the vibration spectrum, respectively.

All results are summarized in Tab. S14 and we only discuss the reactive/non-reactive transition here. Scanning the torsion angles around the single bond connecting the furan rings with the central perfluoro core confirms that for the C5F-derived molecules both open conformations (reactive and non-reactive) are energetically almost indistinguishable (Table S14). In the C4F-case, the non-reactive form is by < 4kcal/mol more stable than the reactive conformer. Nevertheless, due to the small energy differences and reaction barrier height there will be a fast exchange between the two open conformations for all molecular switches in solution and the reactive conformation formed by this pre-equilibrium will then undergo the switching reaction. One additional explanation to the ones given in the main document for the reduced rate of the closing reaction of the C4F compounds (lower quantum yields) compared to C5F is, thus, the smaller concentration of the reactive form (equilibrium is shifted to the non-reactive form).

5. Quantum Mechanical Calculation

Table S14. Absolute (in Hartree) and relative energies (in kcal/mol) of the two open and the closed structures as well as the relevant transition states for C5F-CHO and C4F-CHO and the corresponding thiophene derivates C5F-T-CHO and C5F-T-CHO. The energies are given relative to the energy of the reactive conformer of each molecule.

	C5F-CHO	C4F-CHO	C5F-T-CHO	C4F-T-CHO
non-reactive	-1553.71529680 -0.3015	-1315.91232419 -3.7094	-2199.66055955 0.4835	-1961.85822179 -2.4810
transition state 1	-1553.70881535 3.7657	-1315.89734719 5.6888	-2199.65782964 2.1966	-1961.84658934 4.8185
reactive	-1553.71481636 0.0000	-1315.90641282 0.0000	-2199.66133009 0.0000	-1961.85426806 0.0000
transition state 2	-1553.64047650 46.6490	-1315.82075420 53.7516	-2199.58738919 46.3986	-1961.76852110 53.8070
closed	-1553.68304778 19.9351	-1315.85927027 29.5824	-2199.62923338 20.1410	-1961.80653316 29.9541

CASSCF Calculations:

Due to problems of the DFT approach to describe the homolytic breaking of the bond in the ground state as well as excited energy surfaces we switched to Complete Active Space Multiconfiguration SCF (CASSCF)^[14] calculations for the analysis of the reaction mechanism. Starting from the closed and open form optimized at the CASSCF(10,10)/6-31g level of theory, a relaxed potential energy scan was performed in both directions by increasing and decreasing the C5-C5ⁱ distance to describe the ring opening and closing, respectively. The maximum of the energy along these reaction coordinates was identified and a transition state optimization started. The resulting transition points were then verified by the occurrence of one imaginary frequency and by following the intrinsic reaction coordinate (IRC)^[15] in both directions towards the minimum structure of the closed and open form. For the S₁ state, the same procedure was followed. As starting point of the initial minimization, the corresponding structures of the ground state were used. Thus this minimization corresponds to the transition from the structure reached by the vertical excitation to the corresponding optimum on the excited energy surface (adiabatic excitation).

Even if the process can be nicely followed using the C5-C5ⁱ distance as criterion (see Figure 3 of main document), this distance is not the perfect reaction coordinate. Besides the change in the distance, other degrees of freedom are highly effected by these reactions, which results in the large energy decrease when starting from the vertical excited state (Franck Condon states) without a change in the distance and causes the oscillations of the distance during the optimization of the open form (see also mpeg-animation in the ESI). For the closed forms and the open form of C4F-CHO this relaxation is only slightly changing the distance but leads to

5. Quantum Mechanical Calculation

very different torsion angles of the bond connecting the central ring A with furan (Figs. S12 and S13).

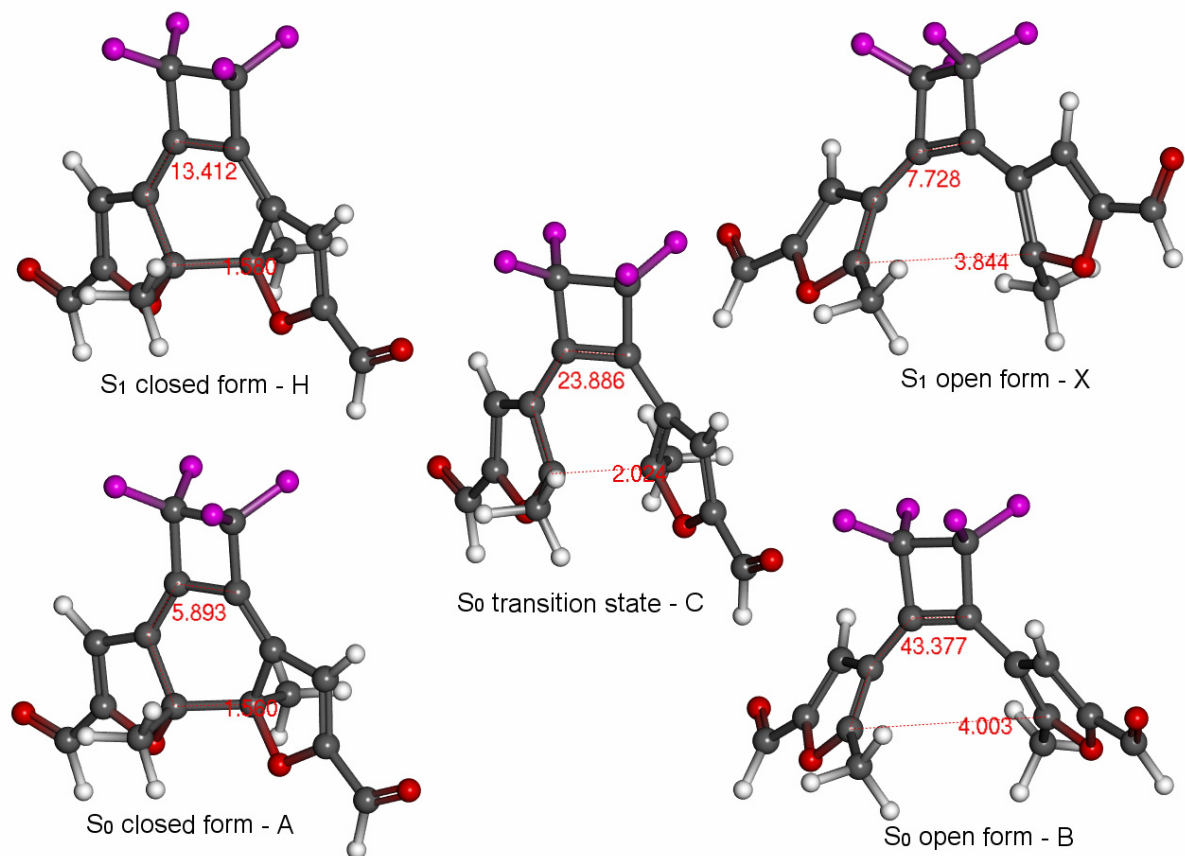


Figure S12. Optimized structures of C4F-CHO: The upper and lower number give the torsion angle (in degree) of the bond connecting the central ring A with the furan and the C5-C5' distance (in Å), respectively. Naming scheme corresponds to Fig. 3 of the main document. A and B corresponds to structures D and E (Franck Condon state), respectively.

5. Quantum Mechanical Calculation

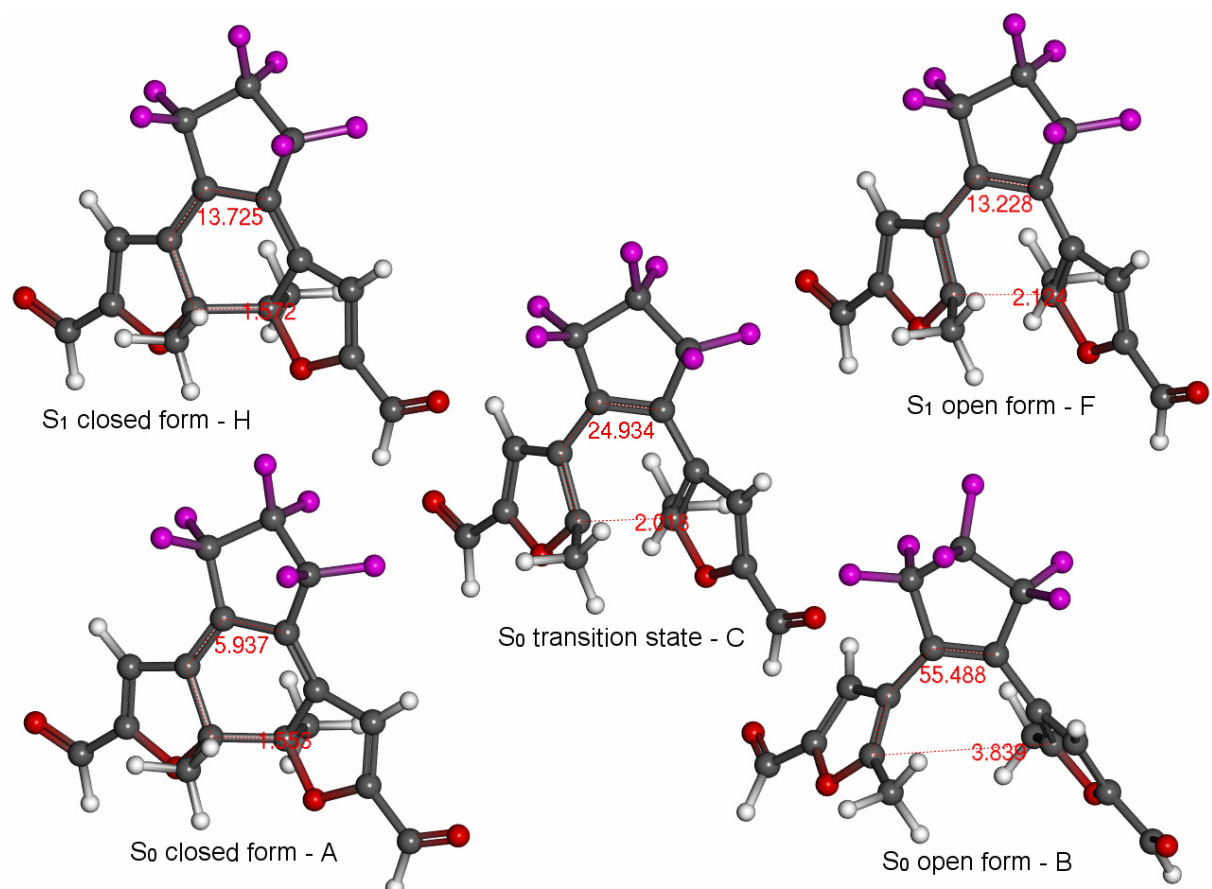


Figure S13. Optimized structures of C5F-CHO: The upper and lower number give the torsion angle (in degree) of the bond connecting the central ring A with the furan and the C5-C5¹ distance (in Å), respectively. Naming scheme corresponds to Fig. 3 of the main document. A and B corresponds to structures D and E (Franck Condon state), respectively.

6. References

1. H. Haarmann, W. Eberbach *Tetrahedron Lett.* 1991, **32**, 903-906.
2. A. Osuka D. Fujikane, H. Shinmori, S. Kobatake, M. Irie, *J. Org. Chem.* 2001, **66**, 3913-3923.
3. G. Gauglitz, *J. Photochem.* 1976, **5**, 41-47.
4. G. Gauglitz, St. Hubig, *J. Photochem.* 1982, **15**, 255-257.
5. H.D. Brauer, R. Schmidt, G. Gauglitz, S. Hubig, *Photochem. Photobiol.* 1983, **37**, 595-598.
6. A.T. Bens, PhD thesis, Heinrich-Heine-Universität, Düsseldorf, Germany, 2001.
7. D. Sysoiev, A. Fedoseev, Y. Kim, T. E. Exner, J. Boneberg, T. Huhn, P. Leiderer, E. Scheer, U. Groth and U. E. Steiner, *Chem.--Eur. J.*, 2011, **17**, 6663-6672.
8. G. M. Sheldrick, SHELX-97, *an integrated system for solving and refining crystal structures from diffraction data; University of Göttingen: Göttingen, Germany*, **1997**.
9. L.J. Farrugia, *J. Appl. Crystallogr.* **1999**, *32*, 837-838.
10. ORTEP-III for Windows, L.J. Farrugia, *J. Appl. Crystallogr.* **1997**, *30*, 565.
11. M. J. Frisch, G. W. Trucks, H. B. Schlegel, G. E. Scuseria, M. A. Robb, J. R. Cheeseman, G. Scalmani, V. Barone, B. Mennucci, G. A. Petersson, H. Nakatsuji, M. Caricato, X. Li, H. P. Hratchian, A. F. Izmaylov, J. Bloino, G. Zheng, J. L. Sonnenberg, M. Hada, M. Ehara, K. Toyota, R. Fukuda, J. Hasegawa, M. Ishida, T. Nakajima, Y. Honda, O. Kitao, H. Nakai, T. Vreven, J. J. A. Montgomery, J. E. Peralta, F. Ogliaro, M. Bearpark, J. J. Heyd, E. Brothers, K. N. Kudin, V. N. Staroverov, R. Kobayashi, J. Normand, K. Raghavachari, A. Rendell, J. C. Burant, S. S. Iyengar, J. Tomasi, M. Cossi, N. Rega, J. M. Millam, M. Klene, J. E. Knox, J. B. Cross, V. Bakken, C. Adamo, J. Jaramillo, R. Gomperts, R. E. Stratmann, O. Yazyev, A. J. Austin, R. Cammi, C. Pomelli, J. W. Ochterski, R. L. Martin, K. Morokuma, V. G. Zakrzewski, G. A. Voth, P. Salvador, J. J. Dannenberg, S. Dapprich, A. D. Daniels, Ö. Farkas, J. B. Foresman, J. V. Ortiz, J. Ciosowski and D. J. Fox, *Gaussian 09, Revision B.01*, (2009) Gaussian, Inc., Wallingford CT.
12. A. D. Becke, *J. Chem. Phys.*, 1993, **98**, 5648-5652.
13. R. Krishnan, J. S. Binkley, R. Seeger and J. A. Pople, *J. Chem. Phys.*, 1980, **72**, 650-654.
14. (a) D. Hegarty and M. A. Robb, *Mol. Phys.* 1979, **38**, 1795-1812. (b) R. H. A. Eade and M. A. Robb, *Chem. Phys. Lett.* 1981, **83**, 362-368. (c) H. B. Schlegel and M. A. Robb, *Chem. Phys. Lett.* 1982, **93**, 43-46. (d) F. Bernardi, A. Bottini, J. J. W. McDougall, M. A. Robb, and H. B. Schlegel, *Far. Symp. Chem. Soc.* 1984, **19**, 137-147. (e) M. J. Frisch, I. N. Ragazos, M. A. Robb, and H. B. Schlegel, *Chem. Phys. Lett.* 1992, **189**, 524-528. (f) N. Yamamoto, T. Vreven, M. A. Robb, M. J. Frisch, and H. B. Schlegel, *Chem. Phys. Lett.* 1996, **250**, 373-378.
15. (a) K. Fukui, *Acc. Chem. Res.* 1981, **14**, 363-368. (b) H. P. Hratchian and H. B. Schlegel, in *Theory and Applications of Computational Chemistry: The First 40 Years*, Ed. C. E. Dykstra, G. Frenking, K. S. Kim, and G. Scuseria (Elsevier, Amsterdam, 2005) 195-249.